Supplementary Figures and Tables

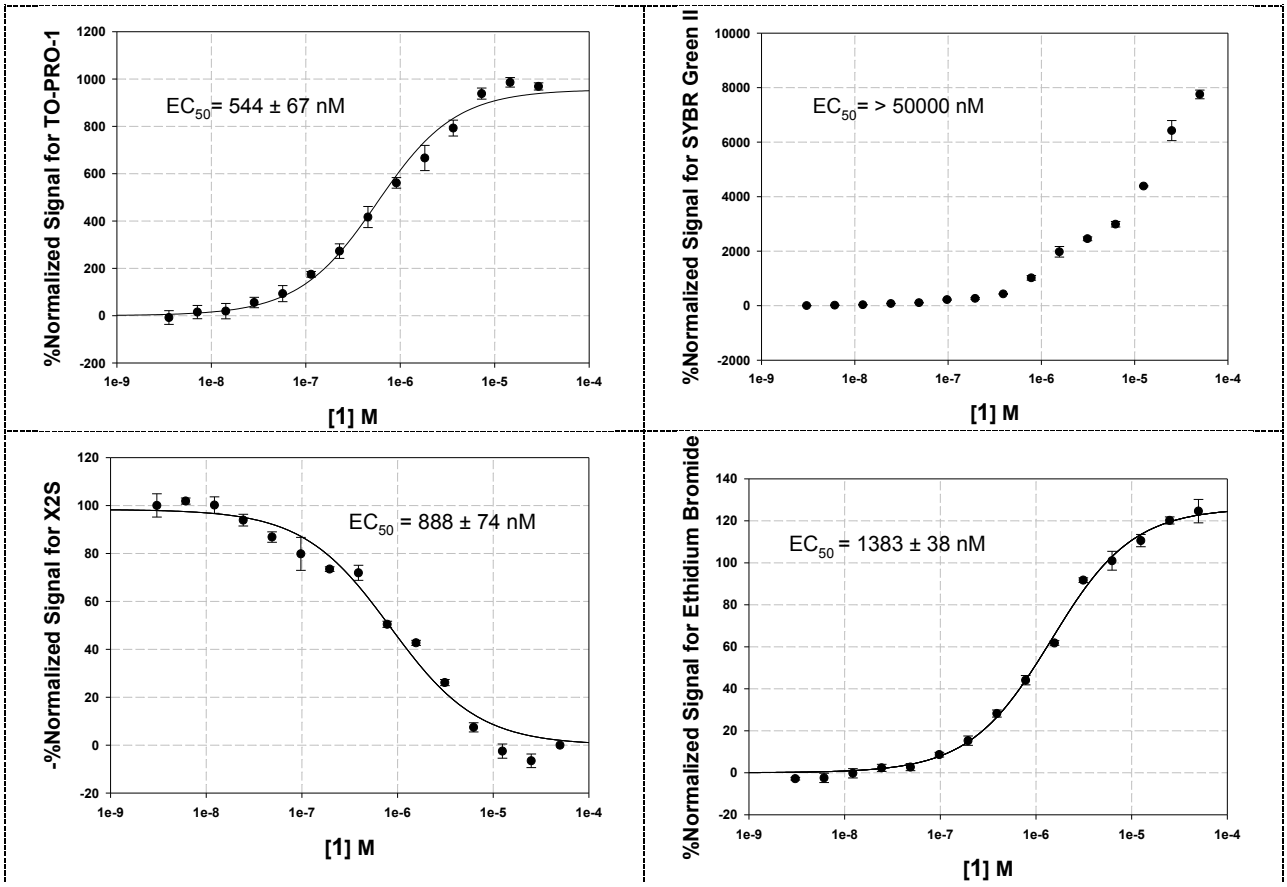

Supplementary Figure S1: Binding curves of TO-PRO-1, SYBR green II, X2S and ethidium bromide to **1**. Each experiment was completed in triplicate, and the error bars are the standard deviations.

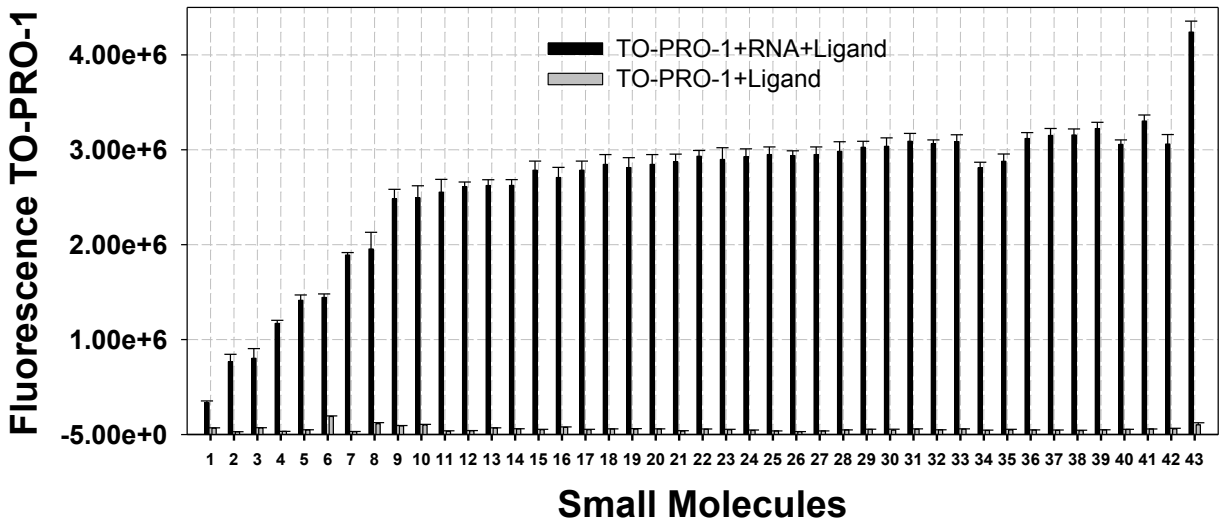

Supplementary Figure S2: High throughput screening by TO-PRO-1 displacement for 6-nucleotide hairpin library (**1**). Each experiment was completed in triplicate, and the error bars are the standard deviations.

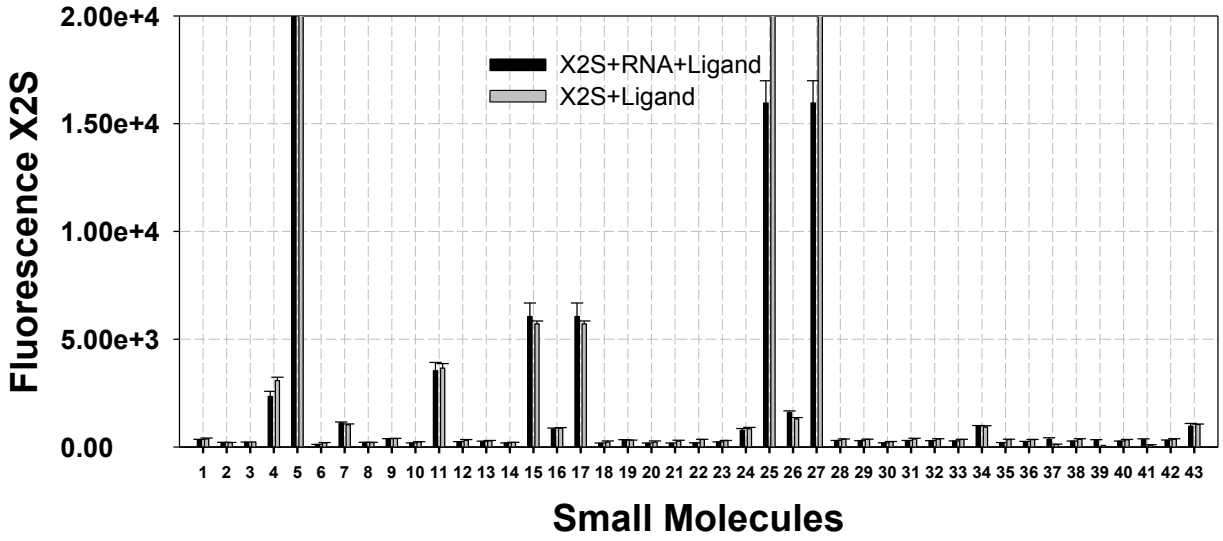

Supplementary Figure S3: High throughput screening by X2S displacement for 6-nucleotide hairpin library (**1**). Each experiment was completed in triplicate, and the error bars are the standard deviations.

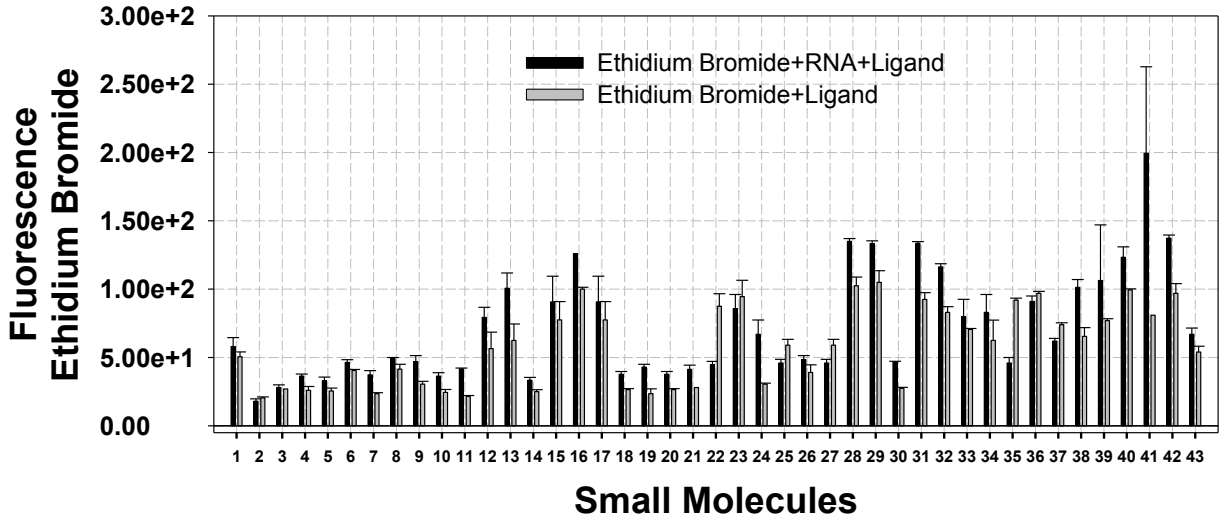

Supplementary Figure S4: High throughput screening by ethidium bromide displacement for 6-nucleotide hairpin library (**1**). Each experiment was completed in triplicate, and the error bars are the standard deviations.

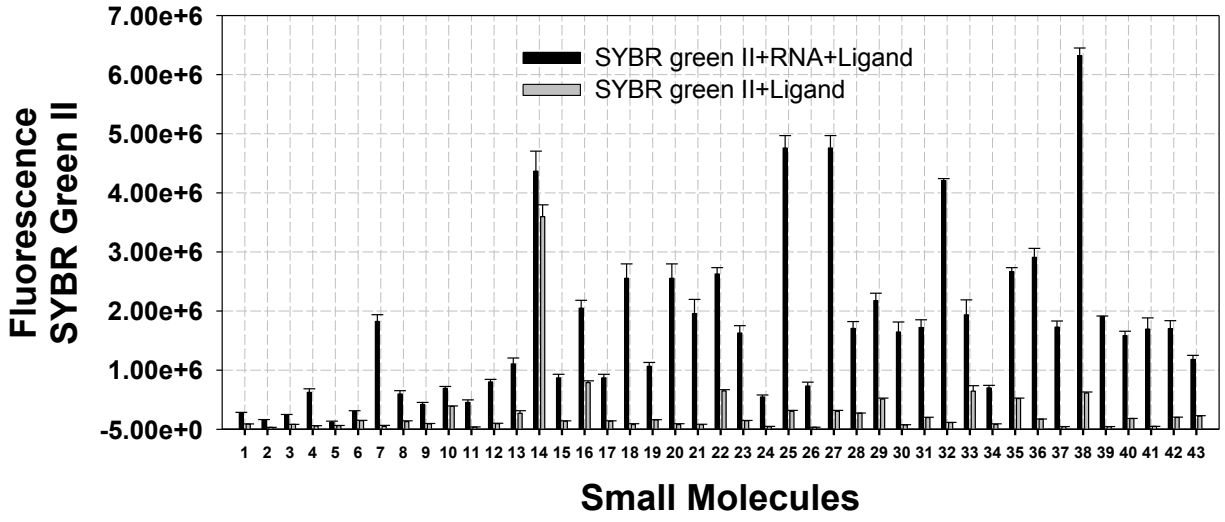

Supplementary Figure S5: High throughput screening by SYBR green II displacement for 6-nucleotide hairpin library (**1**). Each experiment was completed in triplicate, and the error bars are the standard deviations.

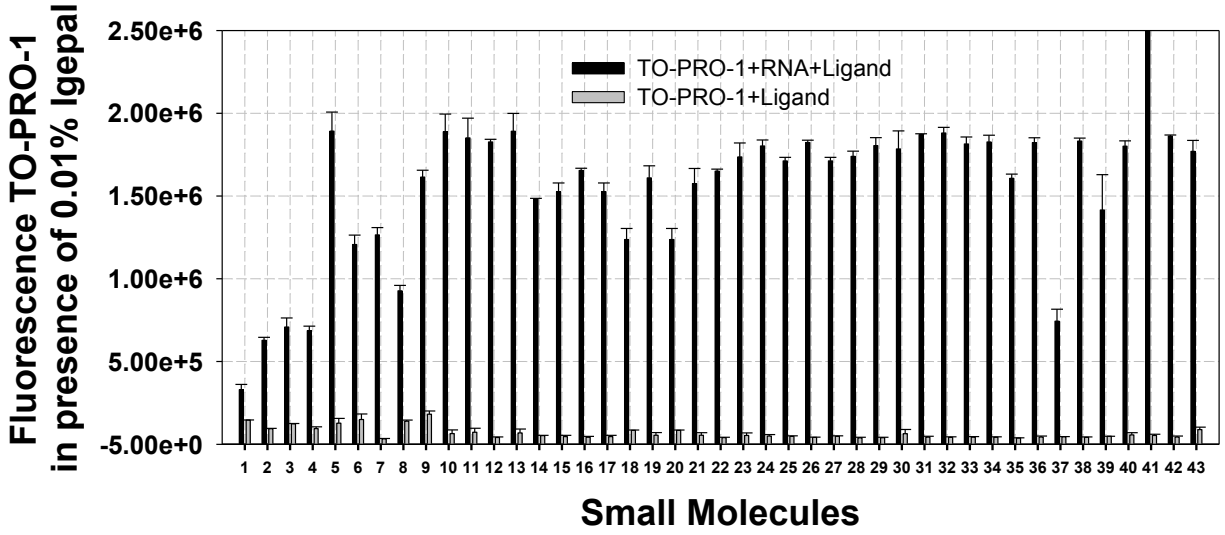

Supplementary Figure S6: High throughput screening by TO-PRO-1 displacement for 6-nucleotide hairpin library (**1**) in presence of 0.01% Igepal. Each experiment was completed in triplicate and the error bars are the standard deviations.

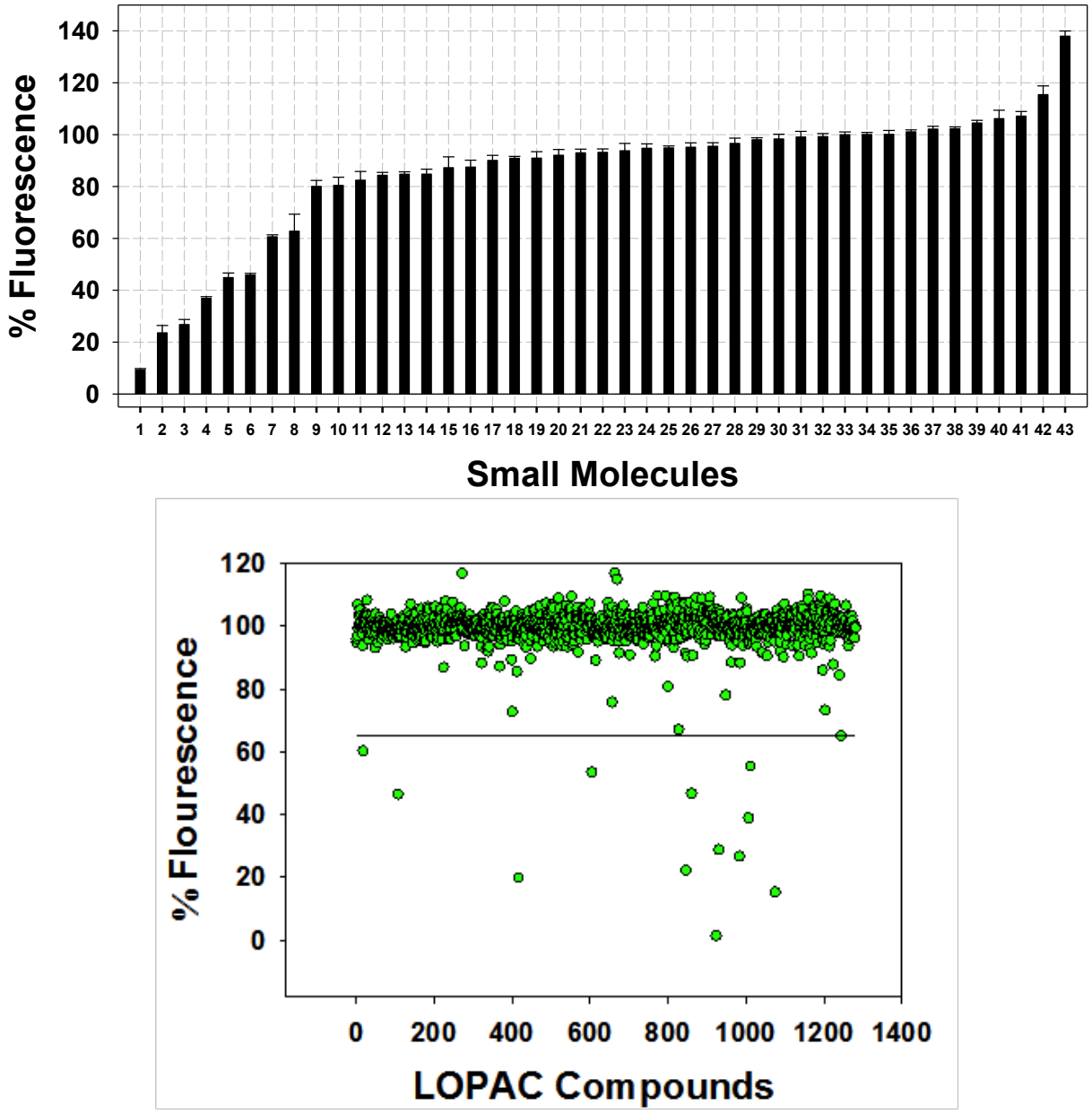

Supplementary Figure S7: High throughput screening by TO-PRO-1 displacement for 6-nucleotide hairpin library (**1**). Each experiment was completed in triplicate, and the error bars are the standard deviations.

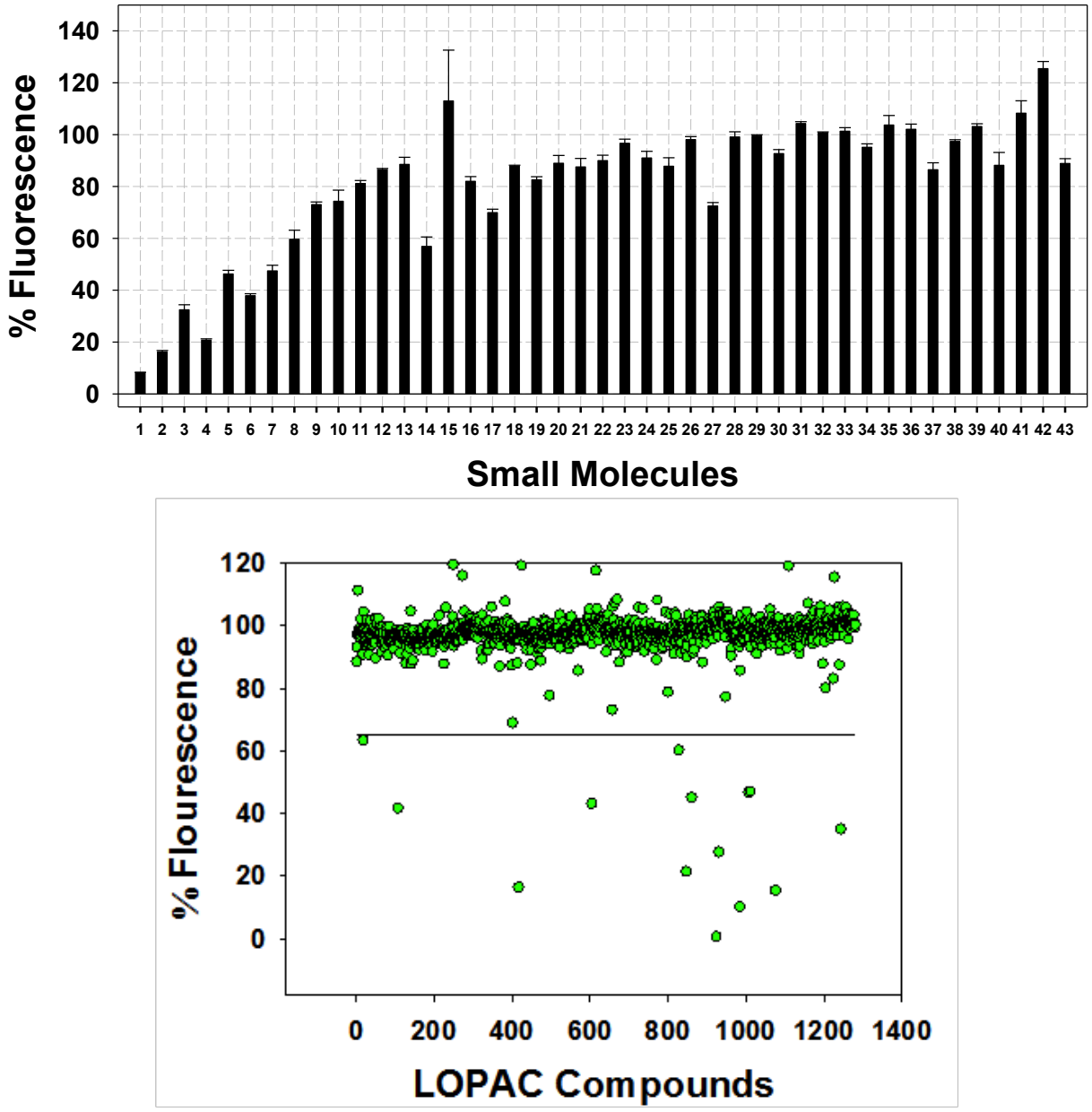

Supplementary Figure S8: High throughput screening by TO-PRO-1 displacement for a 3×2 nucleotide internal loop library (**2**). Each experiment was completed in triplicate, and the error bars are the standard deviations.

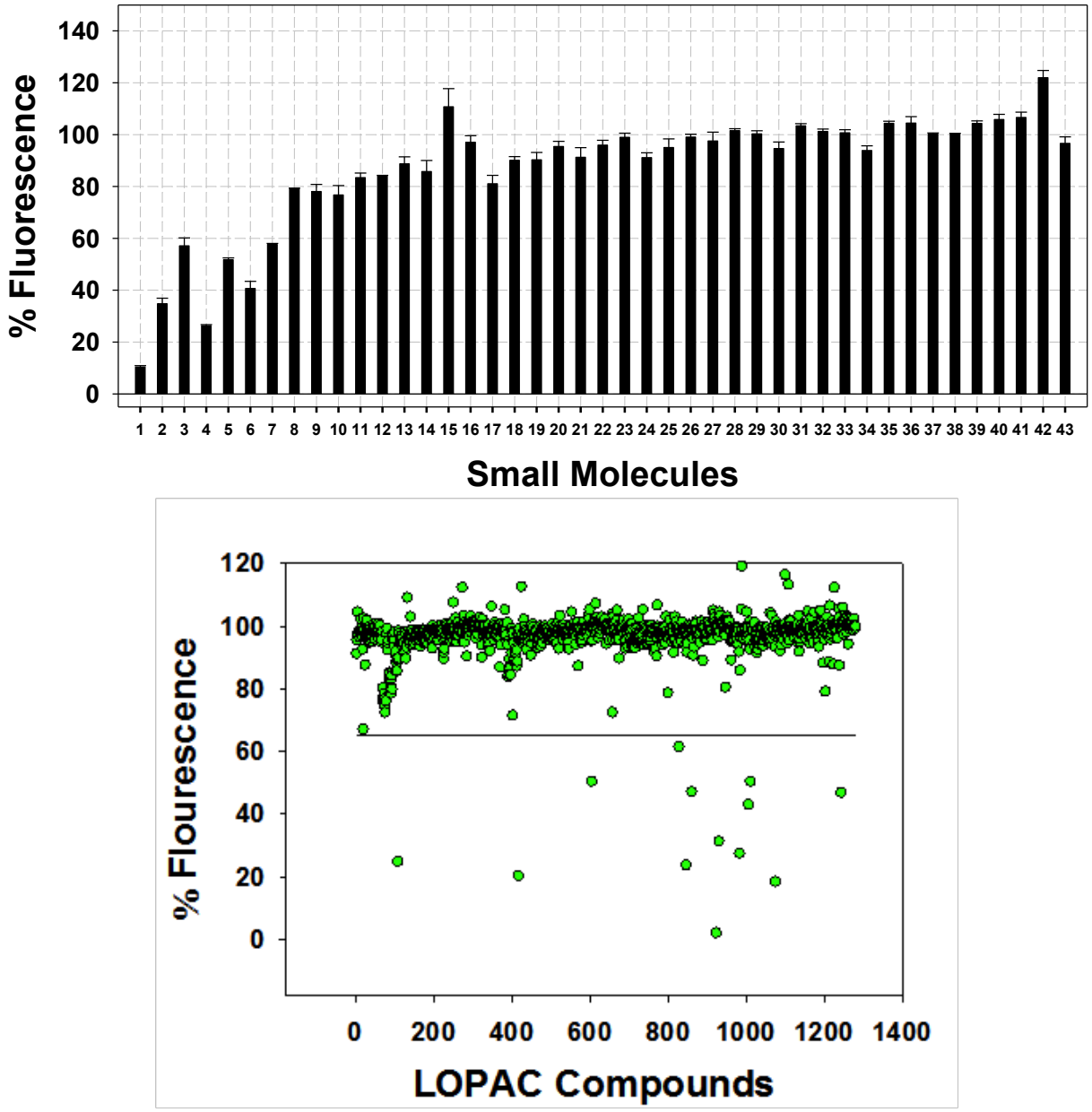

Supplementary Figure S9: High throughput screening by TO-PRO-1 displacement Assay for a 4×4 nucleotide internal loop library (**3**). Each experiment was completed in triplicate and the error bars are the standard deviations.

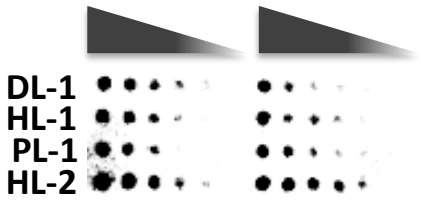

Supplementary Figure S10: Microarray-based screen using tRNA as competitor. Ligands were immobilized onto the slide surface at five different concentrations by reductive amination. The image was obtained after hybridization by with radioactively labeled **1** and excess tRNA (500 times over the number of moles of ligand delivered to the surface and 8,000 times the concentration of **1**).

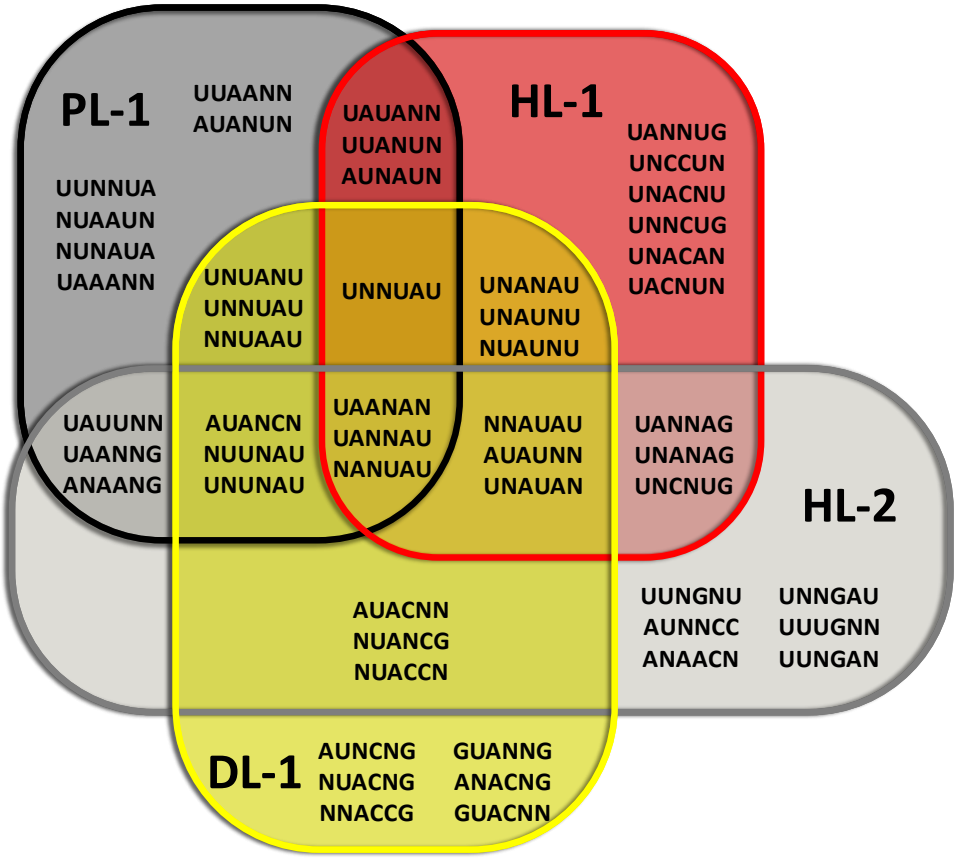

Supplementary Figure S11: Venn Diagram of unique and overlapping statistically significant trends in the RNAs selected to bind **PL-1**, **HL-1**, **DL-1** and **HL-2**. Only four base trends are shown (four fixed bases and two N's). All trends were calculated using the RNA-PSP v. 2.0 program [51] and have a >99% confidence level.

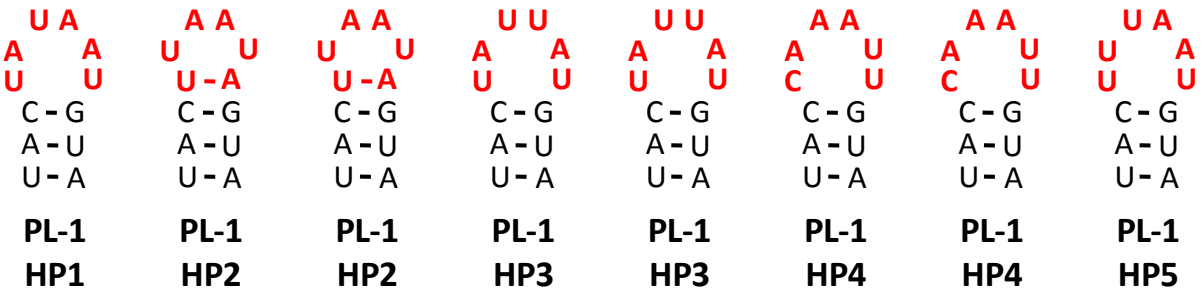
U A
A A
U U
C - G
A - U
U - A
PL-1
HP1
A A
U U
U - A
C - G
A - U
U - A
PL-1
HP2
A A
U U
U - A
C - G
A - U
U - A
PL-1
HP2
U U
A A
U U
C - G
A - U
U - A
PL-1
HP3
U U
A A
U U
C - G
A - U
U - A
PL-1
HP3
A A
A U
C U
C - G
A - U
U - A
PL-1
HP4
A A
A U
C U
C - G
A - U
U - A
PL-1
HP4
U A
U A
U U
C - G
A - U
U - A
PL-1
HP5

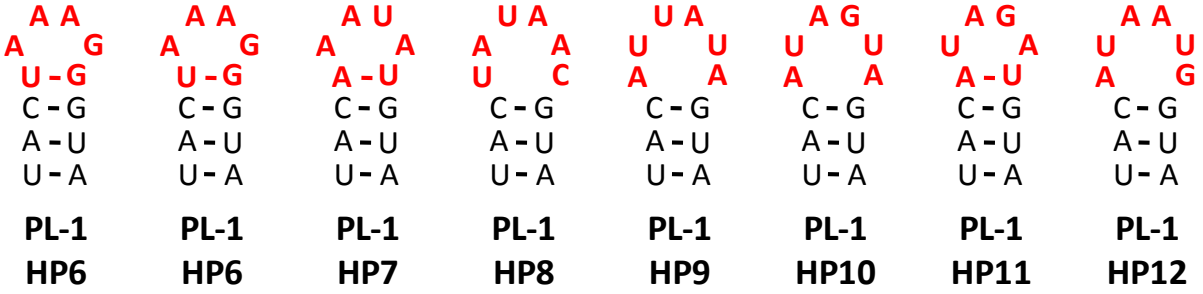
A A
A G
U - G
C - G
A - U
U - A
PL-1
HP6
A A
A G
U - G
C - G
A - U
U - A
PL-1
HP6
A U
A A
A - U
C - G
A - U
U - A
PL-1
HP7
U A
A A
U C
C - G
A - U
U - A
PL-1
HP8
U A
U U
A A
C - G
A - U
U - A
PL-1
HP9
A G
U U
A A
C - G
A - U
U - A
PL-1
HP10
A G
U A
A - U
C - G
A - U
U - A
PL-1
HP11
A A
U U
A G
C - G
A - U
U - A
PL-1
HP12

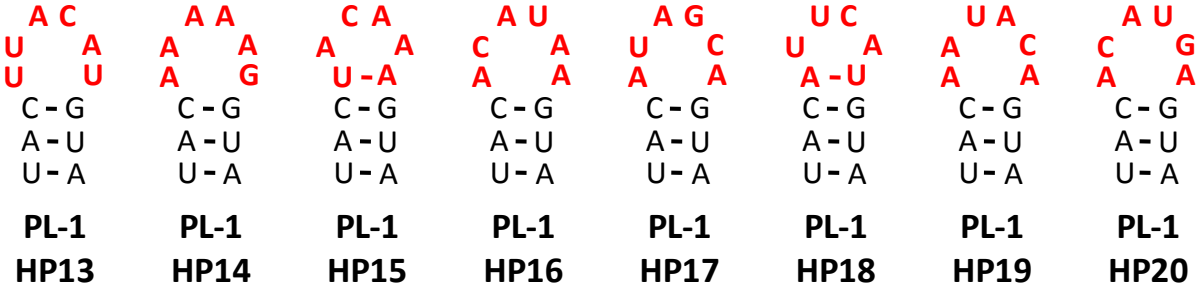
A C
U A
U U
C - G
A - U
U - A
PL-1
HP13
A A
A A
A G
C - G
A - U
U - A
PL-1
HP14
C A
A A
U - A
C - G
A - U
U - A
PL-1
HP15
A U
C A
A A
C - G
A - U
U - A
PL-1
HP16
A G
U C
A A
C - G
A - U
U - A
PL-1
HP17
U C
U A
A - U
C - G
A - U
U - A
PL-1
HP18
U A
A C
A A
C - G
A - U
U - A
PL-1
HP19
A U
C G
A A
C - G
A - U
U - A
PL-1
HP20

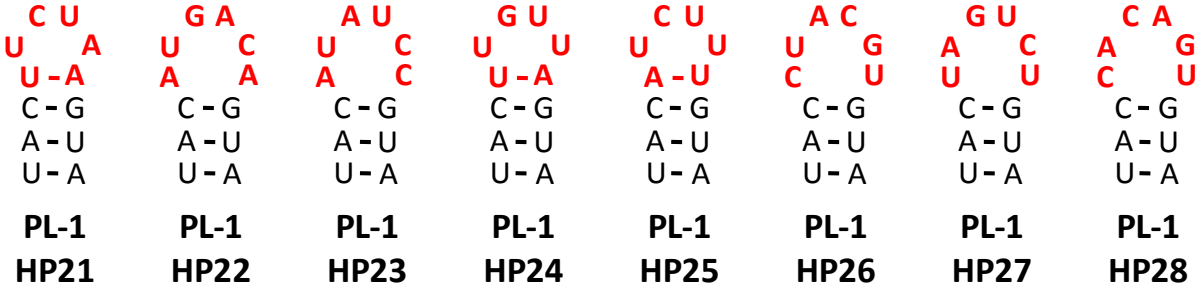
C U
U A
U - A
C - G
A - U
U - A
PL-1
HP21
G A
U C
A A
C - G
A - U
U - A
PL-1
HP22
A U
U C
A C
C - G
A - U
U - A
PL-1
HP23
G U
U U
U - A
C - G
A - U
U - A
PL-1
HP24
C U
U U
A - U
C - G
A - U
U - A
PL-1
HP25
A C
U G
C U
C - G
A - U
U - A
PL-1
HP26
G U
A C
U U
C - G
A - U
U - A
PL-1
HP27
C A
A G
C U
C - G
A - U
U - A
PL-1
HP28

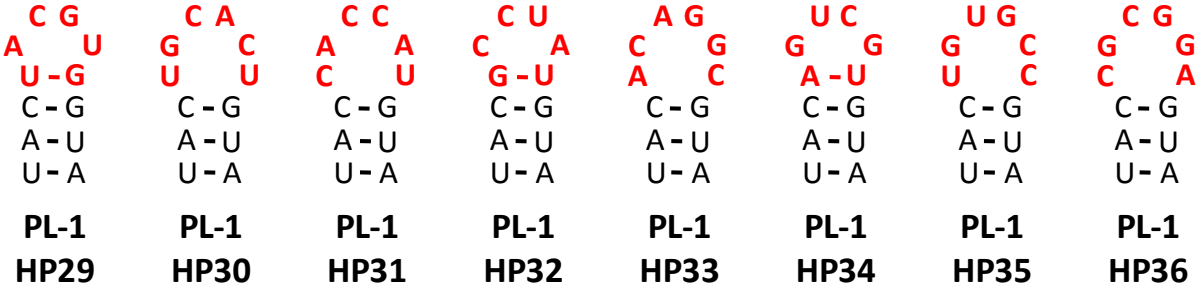
C G
A U
U - G
C - G
A - U
U - A
PL-1
HP29
C A
G C
U U
C - G
A - U
U - A
PL-1
HP30
C C
A A
C U
C - G
A - U
U - A
PL-1
HP31
C U
C A
G - U
C - G
A - U
U - A
PL-1
HP32
A G
C G
A C
C - G
A - U
U - A
PL-1
HP33
U C
G G
A - U
C - G
A - U
U - A
PL-1
HP34
U G
G C
U C
C - G
A - U
U - A
PL-1
HP35
C G
G G
C A
C - G
A - U
U - A
PL-1
HP36

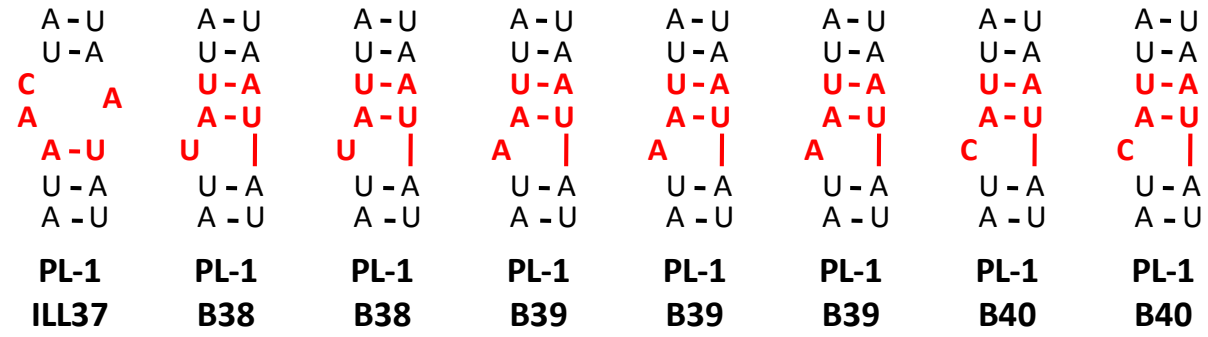

Supplementary Figure S12: Secondary structure of the selected RNA motifs for **PL-1**. Structures are predicted by RNA*structure* program [31]. The red letters in the secondary structures indicate nucleotides that are derived from the randomized region of the libraries; the secondary structure shown is from the boxed nucleotides in Figure 2.

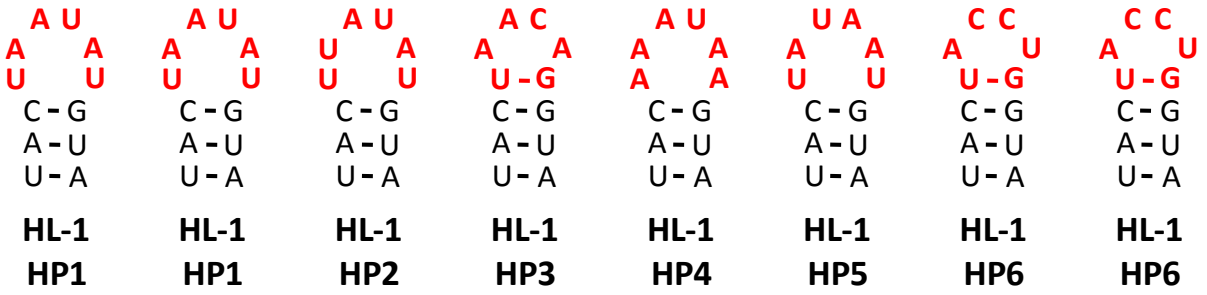
A U
A A
U U
C-G
A-U
U-A
HL-1
HP1
A U
A A
U U
C-G
A-U
U-A
HL-1
HP1
A U
U A
U U
C-G
A-U
U-A
HL-1
HP2
A C
A A
U-G
C-G
A-U
U-A
HL-1
HP3
A U
A A
A A
C-G
A-U
U-A
HL-1
HP4
U A
A A
U U
C-G
A-U
U-A
HL-1
HP5
C C
A U
U-G
C-G
A-U
U-A
HL-1
HP6
C C
A U
U-G
C-G
A-U
U-A
HL-1
HP6
C C
A U
U-G
C-G
A-U
U-A
HL-1
HP6
A C
C A
U U
C-G
A-U
U-A
HL-1
HP7
A C
C A
U U
C-G
A-U
U-A
HL-1
HP7
A G
A A
U-G
C-G
A-U
U-A
HL-1
HP8
A G
A A
U-G
C-G
A-U
U-A
HL-1
HP8
A U
U A
C U
C-G
A-U
U-A
HL-1
HP9
A U
U G
A-U
C-G
A-U
U-A
HL-1
HP10
A C
G A
U U
C-G
A-U
U-A
HL-1
HP11
A A
U U
U U
C-G
A-U
U-A
HL-1
HP12
U A
A C
A-U
C-G
A-U
U-A
HL-1
HP13
C U
U A
U U
C-G
A-U
U-A
HL-1
HP14
A U
U G
A A
C-G
A-U
U-A
HL-1
HP15
U A
A A
U C
C-G
A-U
U-A
HL-1
HP16
C U
A A
A-U
C-G
A-U
U-A
HL-1
HP17
A U
U C
A C
C-G
A-U
U-A
HL-1
HP18
G A
A G
A-U
C-G
A-U
U-A
HL-1
HP19
G A
A G
A-U
C-G
A-U
U-A
HL-1
HP19
U U
U A
A C
C-G
A-U
U-A
HL-1
HP20
A U
U U
U-A
C-G
A-U
U-A
HL-1
HP21
A A
A C
A C
C-G
A-U
U-A
HL-1
HP22
C A
U U
A A
C-G
A-U
U-A
HL-1
HP23
C A
U U
A A
C-G
A-U
U-A
HL-1
HP23
C A
U A
U-G
C-G
A-U
U-A
HL-1
HP24
G A
A A
C U
C-G
A-U
U-A
HL-1
HP25
U U
A G
A C
C-G
A-U
U-A
HL-1
HP26
U G
A C
A A
C-G
A-U
U-A
HL-1
HP27
A U
C C
A G
C-G
A-U
U-A
HL-1
HP28
U A
C A
A C
C-G
A-U
U-A
HL-1
HP29
A C
U C
U-G
C-G
A-U
U-A
HL-1
HP30
A C
C U
A A
C-G
A-U
U-A
HL-1
HP31
U A
G C
A G
C-G
A-U
U-A
HL-1
HP32
G C
U G
G-C
C-G
A-U
U-A
HL-1
HP33

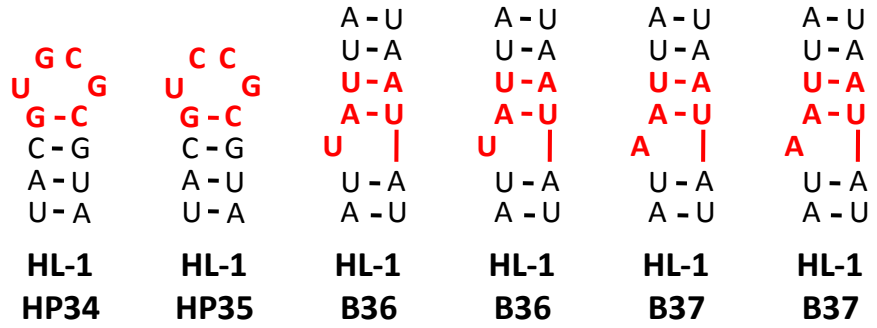

Supplementary Figure S13: Secondary structure of the selected RNA motifs for **HL-1**. Structures are predicted by RNA*structure* program [31]. The red letters in the secondary structures indicate nucleotides that are derived from the randomized region of the libraries; the secondary structure shown is from the boxed nucleotides in Figure 2.

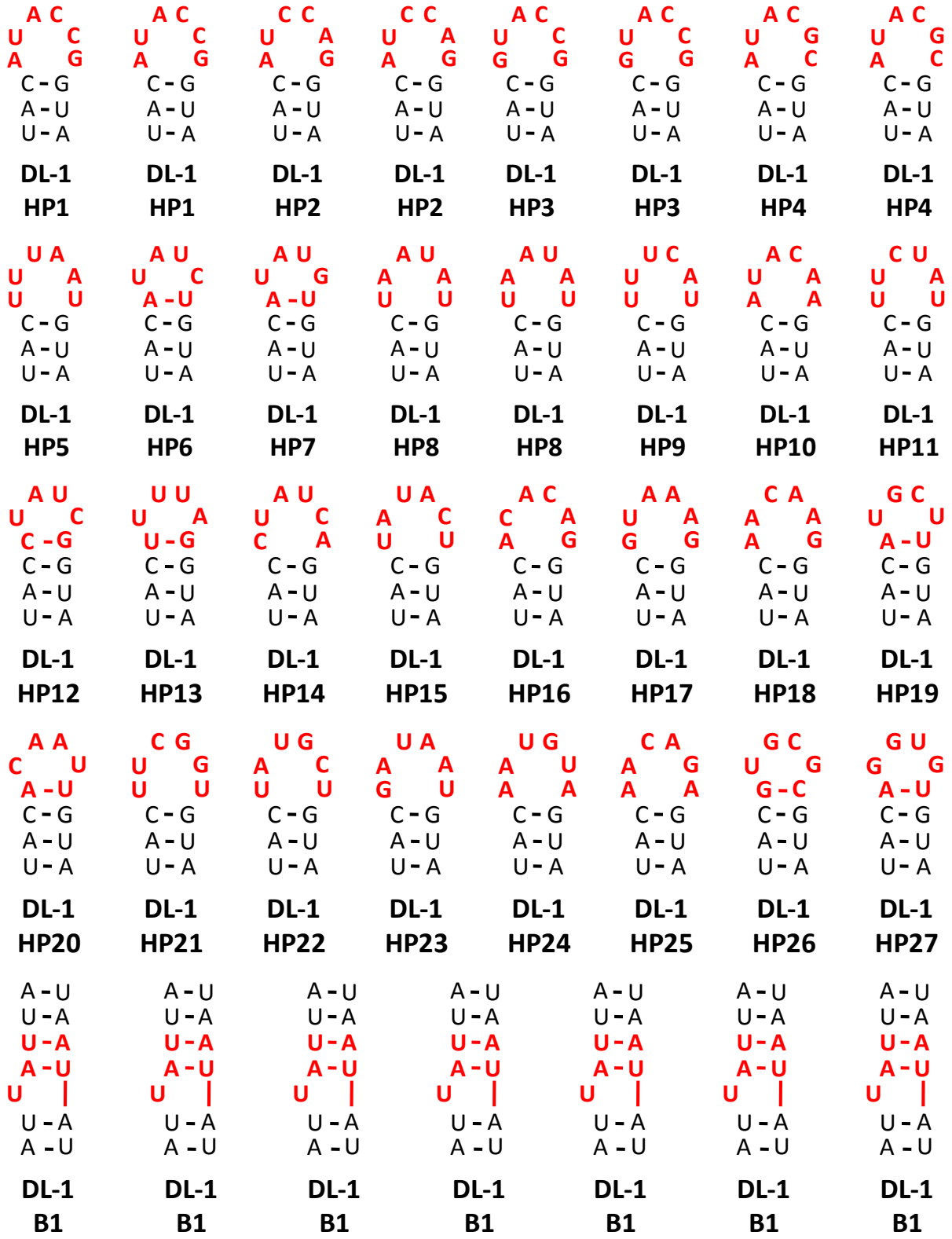
A C
U C
A G
C-G
A-U
U-A
DL-1
HP1
A C
U C
A G
C-G
A-U
U-A
DL-1
HP1
C C
U A
A G
C-G
A-U
U-A
DL-1
HP2
C C
U A
A G
C-G
A-U
U-A
DL-1
HP2
A C
U C
G G
C-G
A-U
U-A
DL-1
HP3
A C
U C
G G
C-G
A-U
U-A
DL-1
HP3
A C
U G
A C
C-G
A-U
U-A
DL-1
HP4
A C
U G
A C
C-G
A-U
U-A
DL-1
HP4
U A
U A
U U
C-G
A-U
U-A
DL-1
HP5
A U
U C
A-U
C-G
A-U
U-A
DL-1
HP6
A U
U G
A-U
C-G
A-U
U-A
DL-1
HP7
A U
A A
U U
C-G
A-U
U-A
DL-1
HP8
A U
A A
U U
C-G
A-U
U-A
DL-1
HP8
U C
U A
U U
C-G
A-U
U-A
DL-1
HP9
A C
U A
A A
C-G
A-U
U-A
DL-1
HP10
C U
U A
U U
C-G
A-U
U-A
DL-1
HP11
A U
U C
C-G
C-G
A-U
U-A
DL-1
HP12
U U
U A
U-G
C-G
A-U
U-A
DL-1
HP13
A U
U C
C A
C-G
A-U
U-A
DL-1
HP14
U A
A C
U U
C-G
A-U
U-A
DL-1
HP15
A C
C A
A G
C-G
A-U
U-A
DL-1
HP16
A A
U A
G G
C-G
A-U
U-A
DL-1
HP17
C A
A A
A G
C-G
A-U
U-A
DL-1
HP18
G C
U U
A-U
C-G
A-U
U-A
DL-1
HP19
A A
C U
A-U
C-G
A-U
U-A
DL-1
HP20
C G
U G
U U
C-G
A-U
U-A
DL-1
HP21
U G
A C
U U
C-G
A-U
U-A
DL-1
HP22
U A
A A
G U
C-G
A-U
U-A
DL-1
HP23
U G
A U
A A
C-G
A-U
U-A
DL-1
HP24
C A
A G
A A
C-G
A-U
U-A
DL-1
HP25
G C
U G
G-C
C-G
A-U
U-A
DL-1
HP26
G U
G G
A-U
C-G
A-U
U-A
DL-1
HP27
A-U
U-A
U-A
A-U
U |
U-A
A-U
DL-1
B1
A-U
U-A
U-A
A-U
U |
U-A
A-U
DL-1
B1
A-U
U-A
U-A
A-U
U |
U-A
A-U
DL-1
B1
A-U
U-A
U-A
A-U
U |
U-A
A-U
DL-1
B1
A-U
U-A
U-A
A-U
U |
U-A
A-U
DL-1
B1
A-U
U-A
U-A
A-U
U |
U-A
A-U
DL-1
B1
A-U
U-A
U-A
A-U
U |
U-A
A-U
DL-1
B1

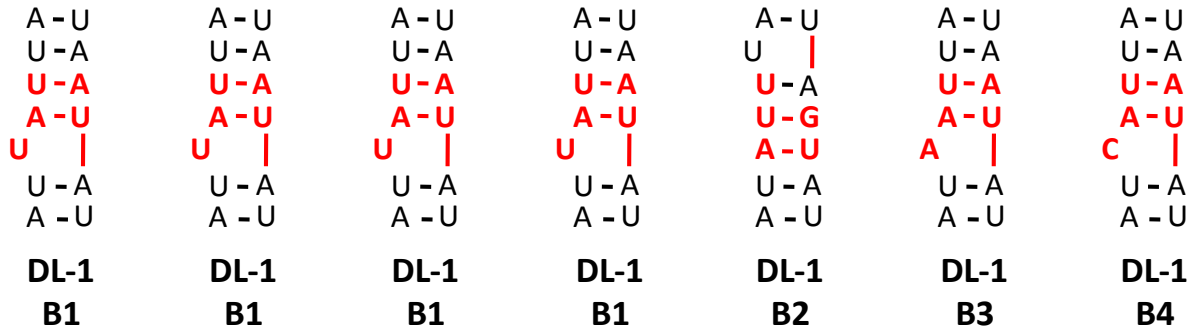

Supplementary Figure S14: Secondary structure of the selected RNA motifs for **DL-1**. Structures are predicted by RNA*structure* program [31]. The red letters in the secondary structures indicate nucleotides that are derived from the randomized region of the libraries; the secondary structure shown is from the boxed nucleotides in Figure 2.

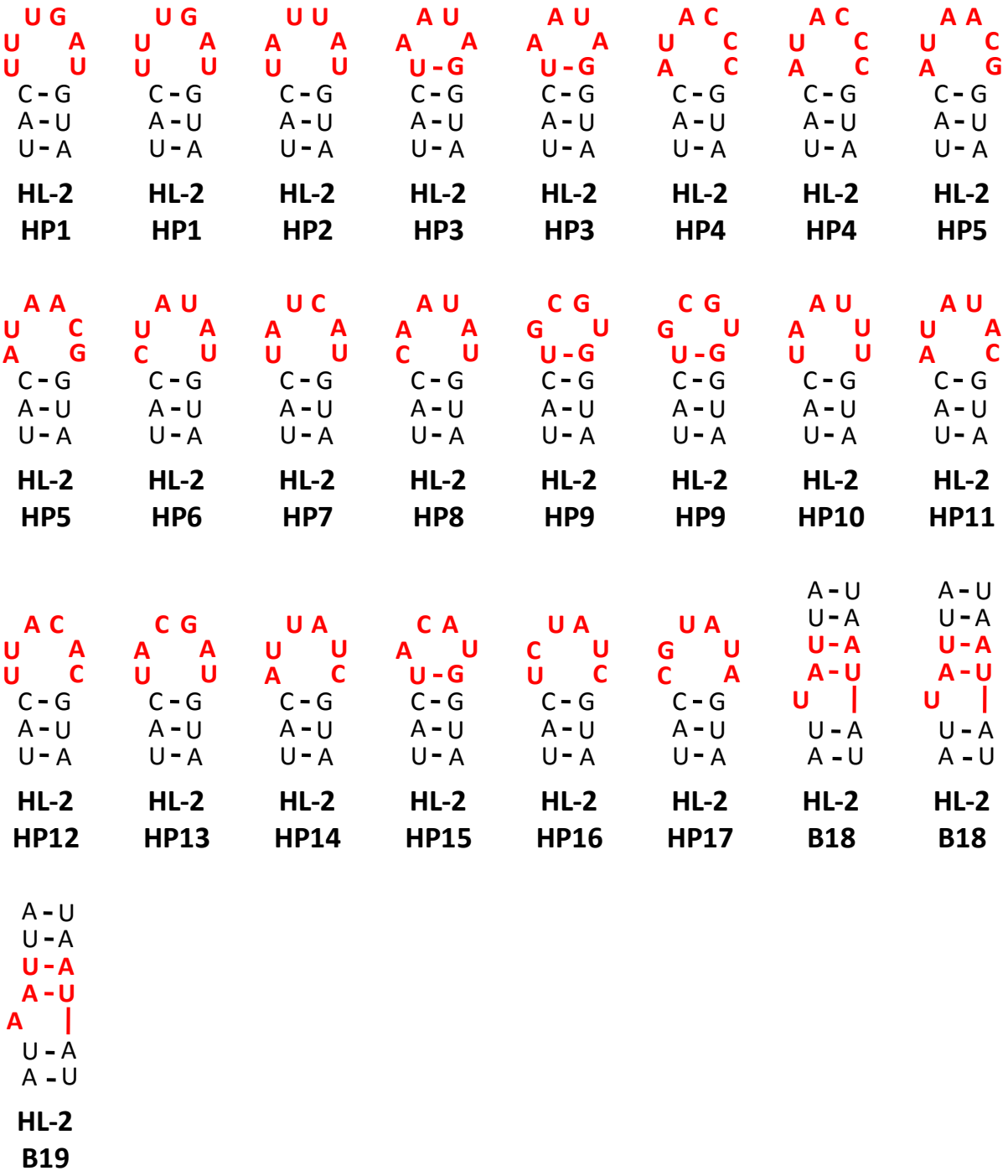

Supplementary Figure S15: Secondary structure of the selected RNA motifs for **PL-1**. Structures are predicted by RNA*structure* program [31]. The red letters in the secondary structures indicate nucleotides that are derived from the randomized region of the libraries; the secondary structure shown is from the boxed nucleotides in Figure 2.

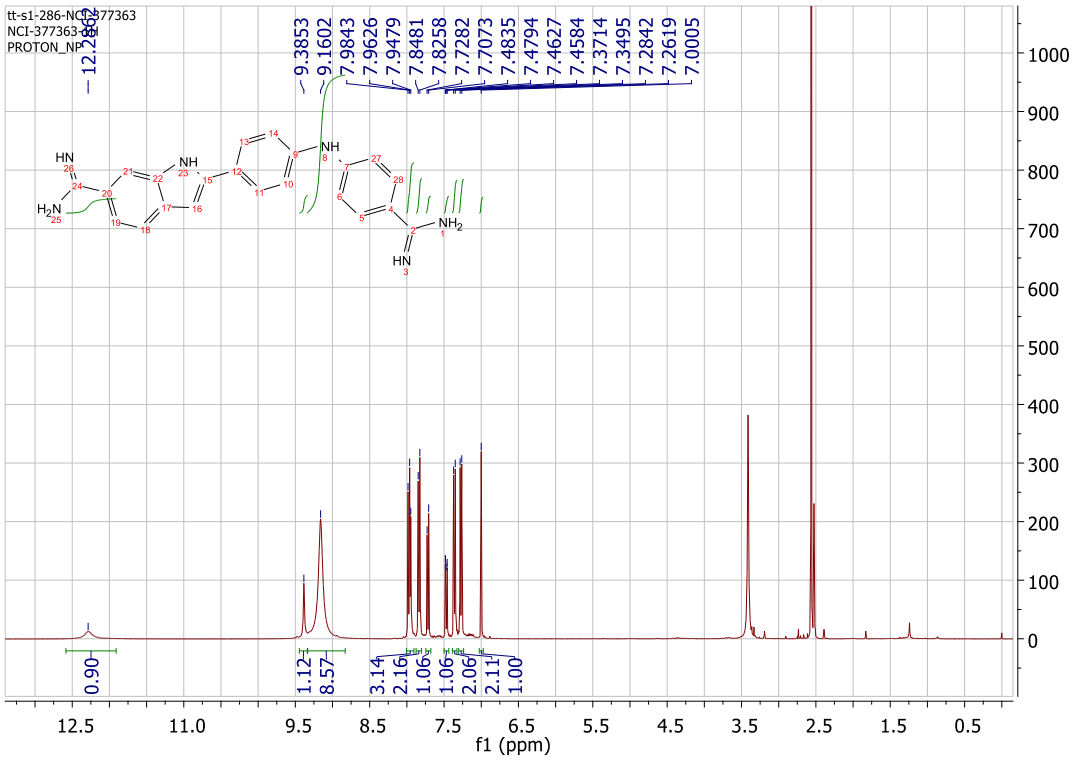
tt-s1-286-NCI-377363
NCI-377363-1H
PROTON_NP
12.2662
9.3853
9.1602
7.9843
7.9626
7.9479
7.8481
7.8258
7.7282
7.7073
7.4835
7.4794
7.4627
7.4584
7.3714
7.3495
7.2842
7.2619
7.0005
0.90
1.12
8.57
3.14
2.16
1.06
1.06
2.06
2.11
1.00
f1 (ppm)

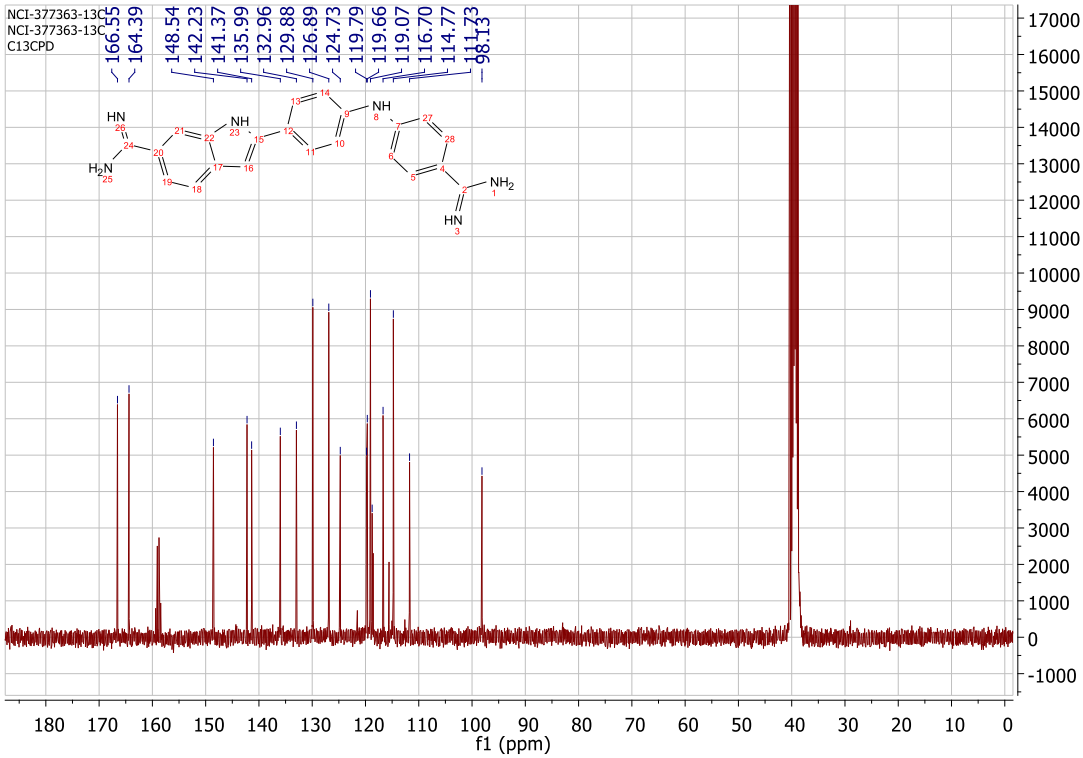
NCI-377363-13C
NCI-377363-13C
C13CPD
166.55
164.39
148.54
142.23
141.37
135.99
132.96
129.88
126.89
124.73
119.79
119.66
119.07
116.70
114.77
111.73
98.13
f1 (ppm)

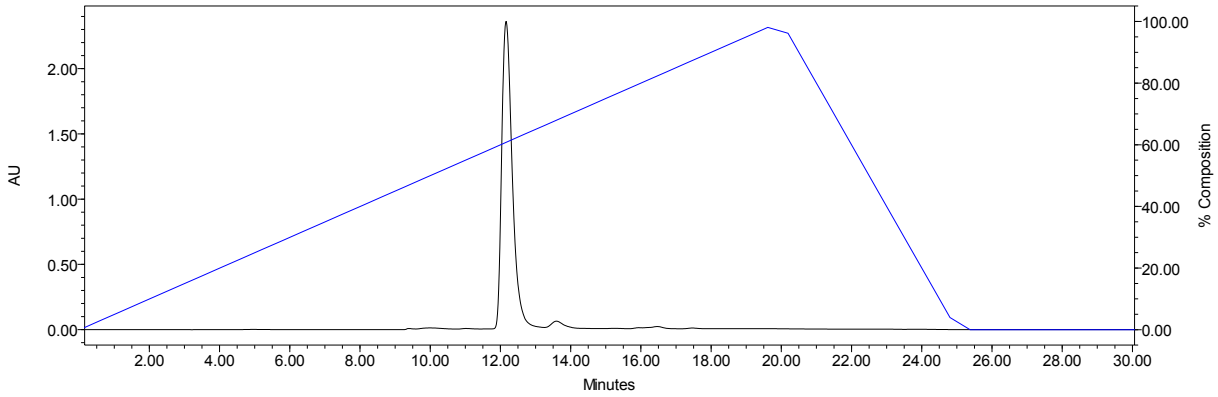

Supplementary Figure S16: ^{1}H NMR spectrum, ^{13}C NMR spectrum and analytical HPLC of **PL-1.** The purity of **PL-1** was determined by reverse phase HPLC using a gradient of 0-100% MeOH in water over 20 min; t_R= 12 min. MS-ESI(+) HRMS: calculated: 369.1822 ($M + H^+$); observed: 369.1826 ($M + H^+$). ^{1}H NMR (DMSO-D_6, 400 MHz) δ 7.00 (1H, s), 7.27 (2H, d, J=9 Hz), 7.36 (2H, d, J=9 Hz), 7.47 (1H, d, J=8 Hz), 7.72 (1H, d, J=9 Hz), 7.84 (2H, d, J=9 Hz), 7.96 (3H, m), 9.16 (9H, bd), 9.39 (1H, s), 12.29 (1H, s). ^{13}C NMR (DMSO-D_6, 100 MHz) δ 98.13, 111.73, 114.77, 116.70, 118.75, 119.07, 119.66, 119.79, 124.73, 126.89, 129.88, 132.96, 135.99, 141.37, 142.23, 148.54, 164.39, 166.55.

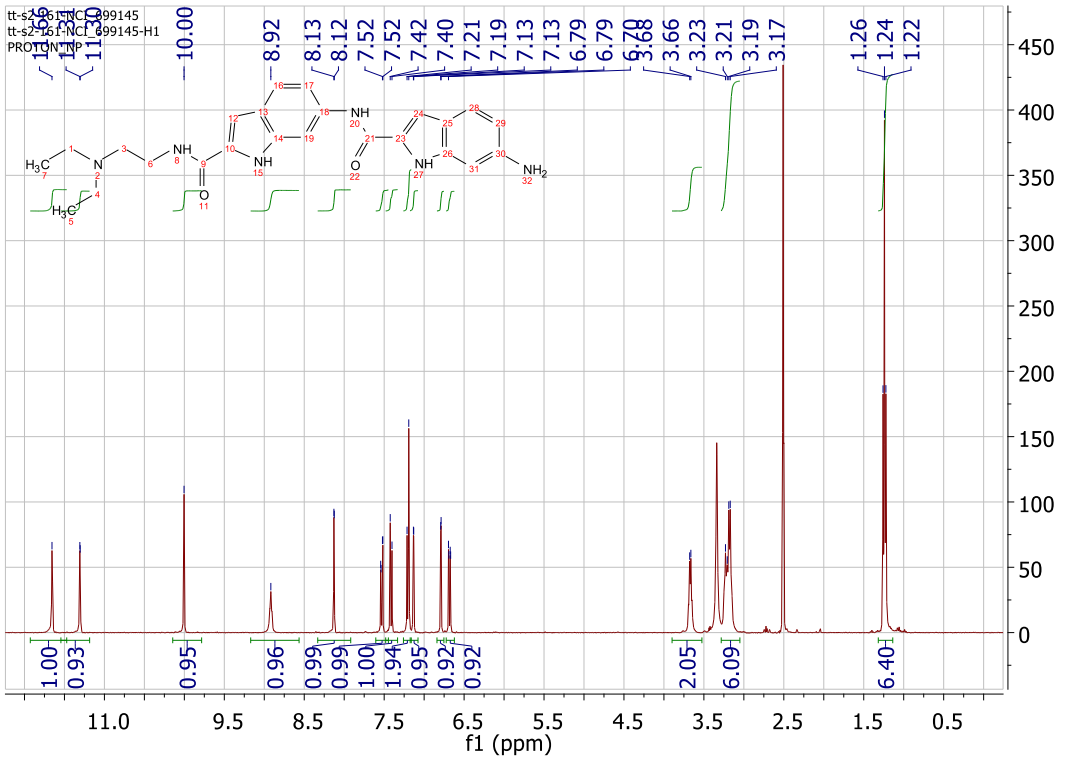
tt-s2-161-NCI_699145
tt-s2-161-NCI_699145-H1
PROTON_NP
f1 (ppm)

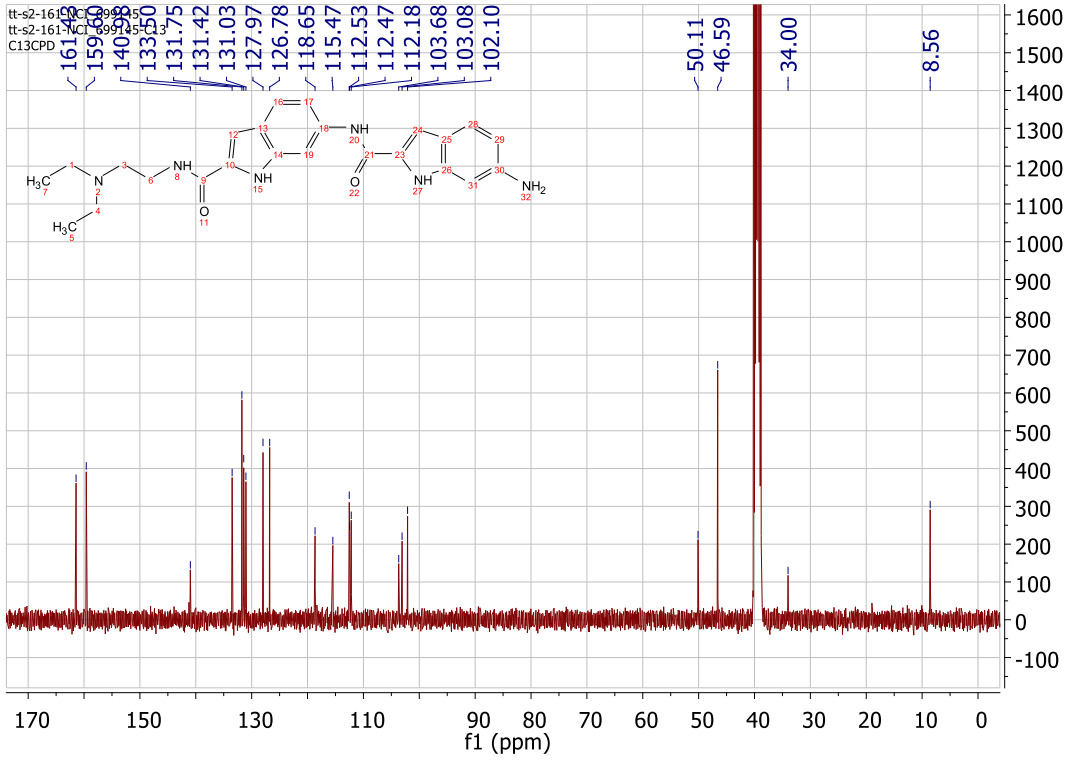
tt-s2-161-NCI_699145
tt-s2-161-NCI_699145-C13
C13CPD
f1 (ppm)

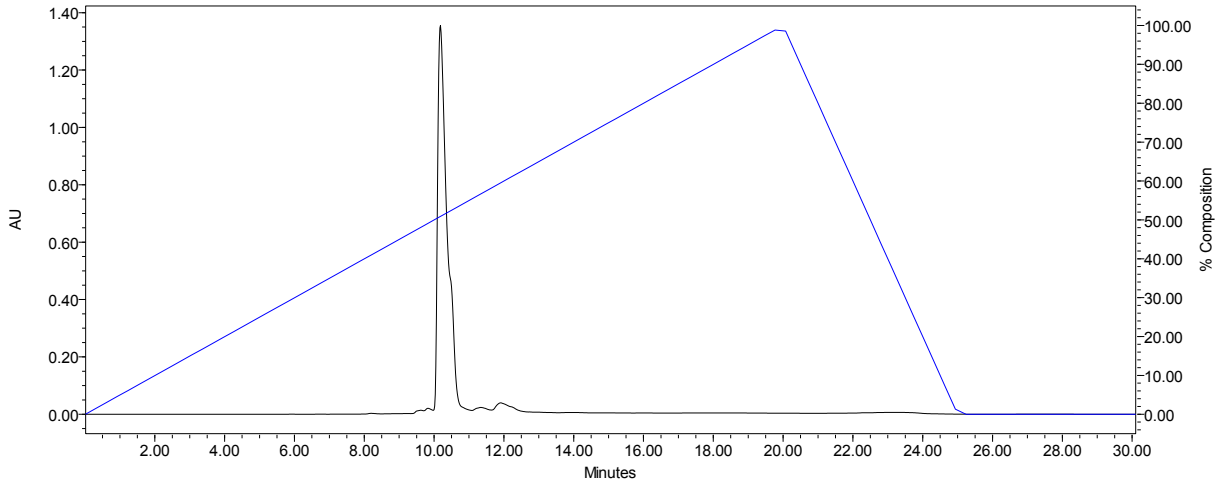

Supplementary Figure S17: ^{1}H NMR spectrum, ^{13}C NMR spectrum and analytical HPLC of **HL-1.** The purity of **HL-1** was determined by reverse phase HPLC using a gradient of 0-100% MeOH in water over 20 min; t_R= 11 min. MS-ESI(+) HRMS: calculated: 433.2352 (M + H^+); observed: 433.2350 (M + H^+). ^{1}H NMR (DMSO-D_6, 400 MHz) δ 1.24 (6H, t, J=8 Hz), 3.18 (4H, q, J=8 Hz), 3.23 (2H, t, J=8 Hz), 3.67 (2H, q, J=9 Hz), 6.68 (1H, d, J=12 Hz), 6.79 (1H, s), 7.13 (1H, s), 7.19 (1H, s), 7.20 (1H, d, J=8 Hz), 7.41 (1H, d, J=8 Hz), 7.53 (1H, d, J=8 Hz), 8.12 (1H, s), 9.82 (1H, t, J=4 Hz), 10.00 (1H, s), 11.30 (1H, s), 11.66 (1H, s). ^{13}C NMR (DMSO-D_6, 100 MHz) δ 8.56, 34.00, 46.59, 50.11, 102.10, 103.08, 103.68, 112.18, 112.47, 112.53, 115.47, 118.65, 126.78, 127.97, 131.03, 131.42, 131.75, 133.50, 140.98, 159.60, 161.43.

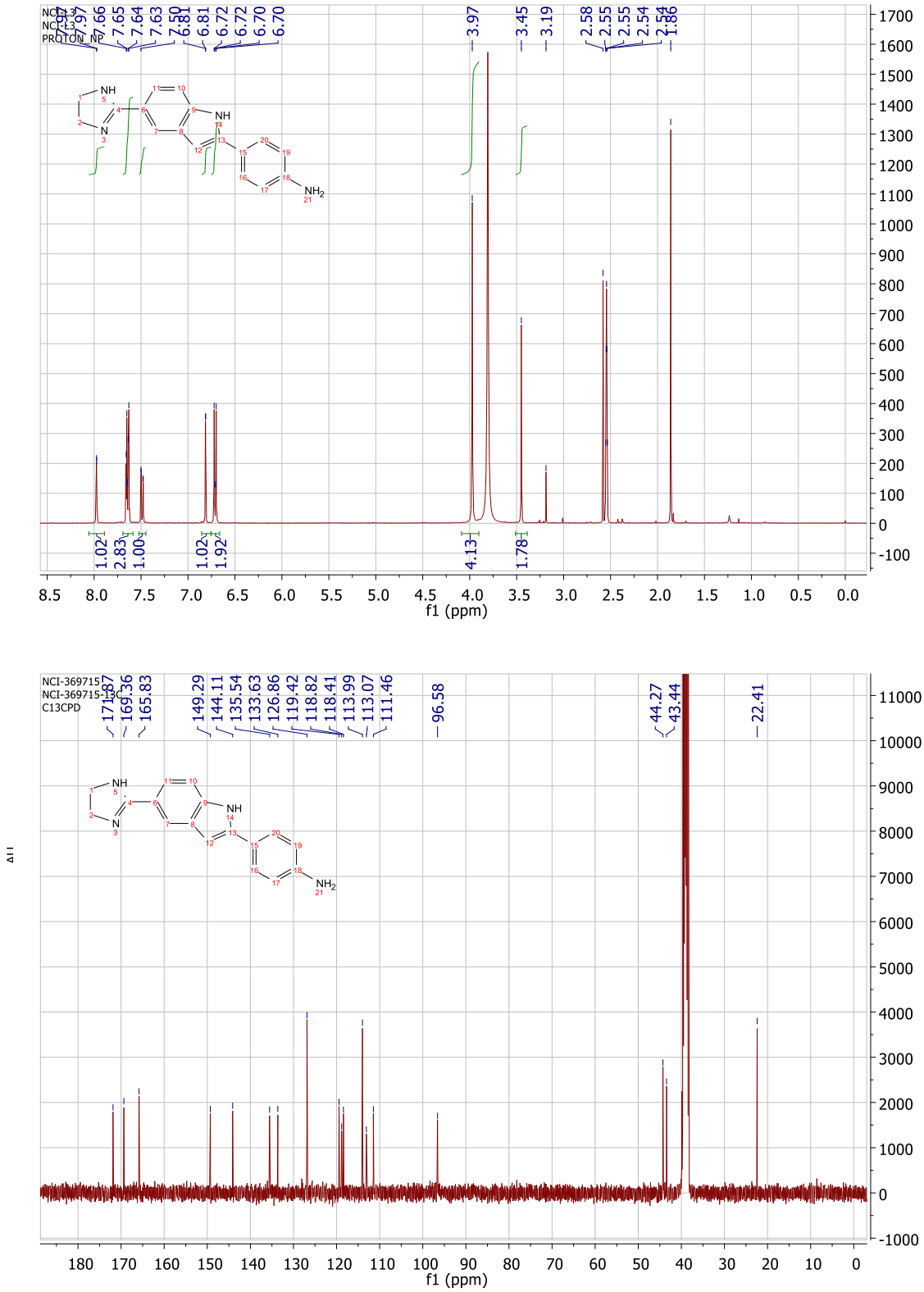

Supplementary Figure S18: ^{1}H NMR spectrum, ^{13}C NMR spectrum and analytical HPLC of **DL-1.** The purity of **DL-1** was determined by reverse phase HPLC using a gradient of 0-100% MeOH in water over 20 min; t_R= 6 min. MS-ESI(+) HRMS: calculated: 277.1448 (M +

H^+); observed: 277.1449 (M + H^+). ^1H NMR (DMSO-D_6, 400 MHz) δ 3.45 (2H, s), 3.97 (4H, s), 6.71 (2H, d, J=9 Hz), 6.81 (1H, s), 7.49 (1H, d, J=8 Hz), 7.63-7.65 (3H, m), 7.97 (1H, s). ^{13}C NMR (DMSO-D_6, 100 MHz) δ 43.44, 44.27, 96.58, 111.46, 113.07, 113.99, 118.41, 118.81, 119.42, 126.86, 133.63, 135.54, 144.11, 149.29, 165.83, 169.36, 171,87.

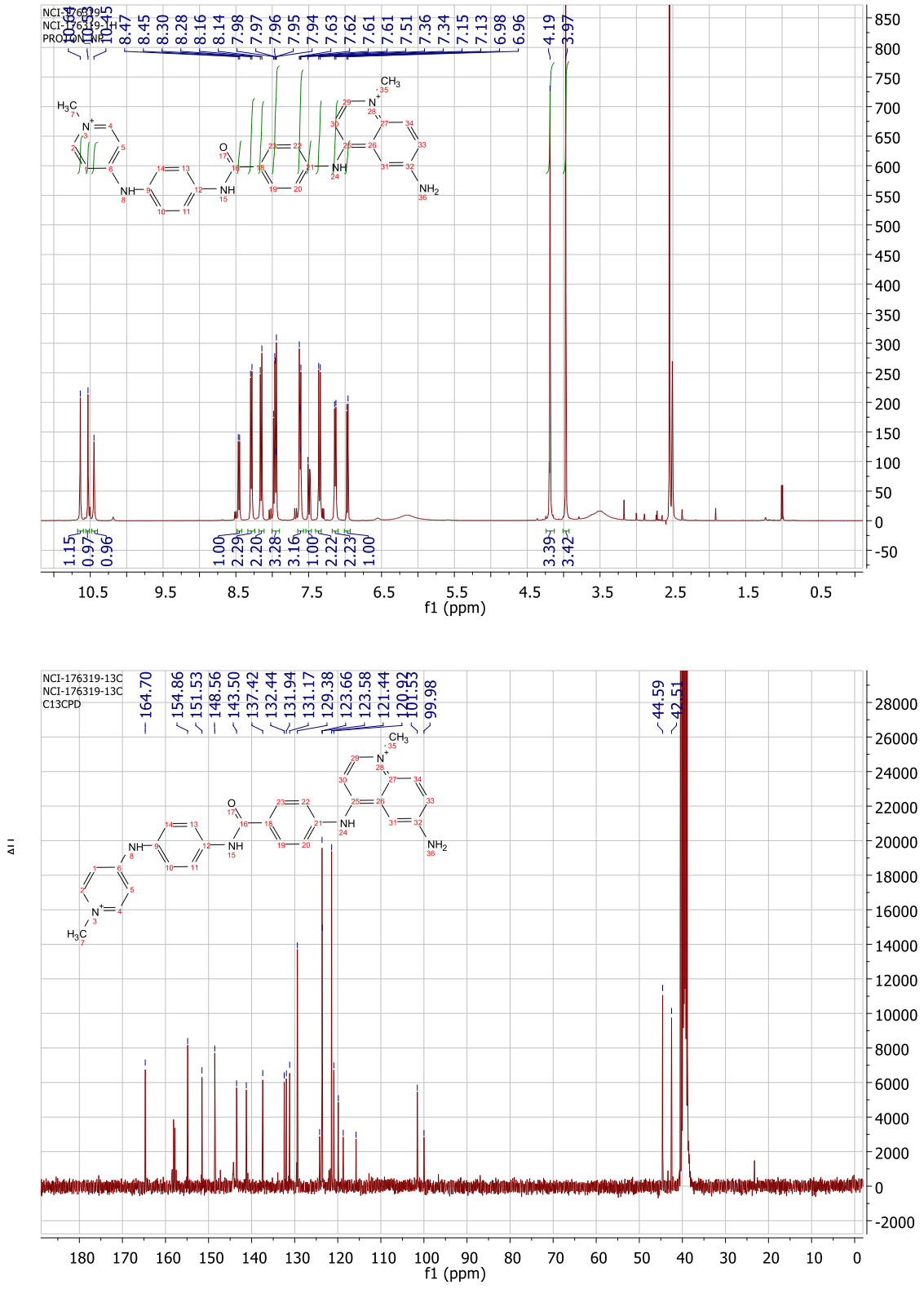

Supplementary Figure S19: ^{1}H NMR spectrum, ^{13}C NMR spectrum and analytical HPLC of **HL-2.** The purity of **HL-2** was determined by reverse phase HPLC using a gradient of 0-

100% MeOH in water over 20 min; t_R= 11.5 min. MS-ESI(+) HRMS: calculated: 475.2241 ($M - H^+$); observed: 475.2235 ($M - H^+$). ^1H NMR (DMSO-D_6, 400 MHz) δ 3.97 (3H, s), 4.19 (3H, s), 6.97 (1H, d, J=7 Hz), 7.14 (2H, d, J=7 Hz), 7.35 (2H, d, J=9 Hz), 7.51 (1H, d, J=7 Hz), 7.62 (3H, m), 7.96 (3H, m), 8.15 (2H, d, J=9 Hz), 8.29 (2H, d, J=7 Hz), 8.46 (1H, d, J=7 Hz), 10.45 (1H,s), 10.53 (1H, s), 10.64 (1H, s). ^{13}C NMR (DMSO-D_6, 100 MHz) δ 42.51, 44.59, 99.98, 101.53, 115.57, 118.74, 119.86, 120.92, 121.44, 123.58, 123.66, 124.22, 129.38, 131.17, 131.94, 132.94, 137.42, 141.24, 143.50, 148.56, 151.53, 154.86, 164.70.

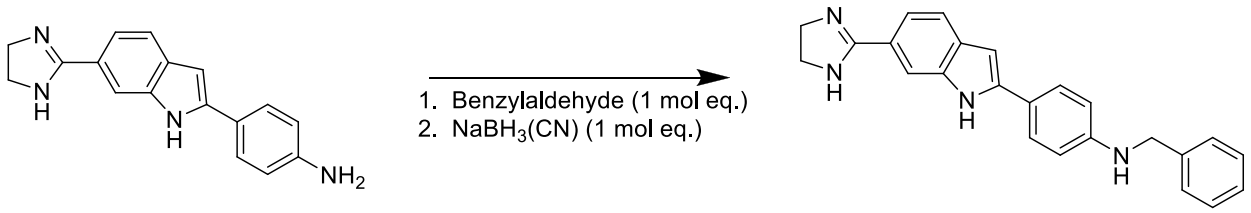

Supplementary Figure S20: Scheme for the synthesis of ***N*-benzyl-4-(6-(4,5-dihydro-1*H*-imidazol-2-yl)-1*H*-indol-2-yl)aniline** (**DL-1 Benzyl**). 4-(6-(4,5-dihydro-1*H*-imidazol-2-yl)-1*H*-indol-2-yl)aniline (**DL-1)** (20 µmol in 400 µL DMSO) was diluted in 2 mL of ethanol. Distilled benzaldehyde (20 µmol) was added, and the mixture was stirred at room temperature for 30 min. $NaCNBH_3$ (20 µL of 1 M solution in water) was then added, and the mixture was stirred at room temperature for 12 h. The formation of **DL-1 Benzyl** was confirmed by ESI-MS and purified by reverse phase HPLC using a gradient of 0-100% MeOH in water over 60 min (90% yield).

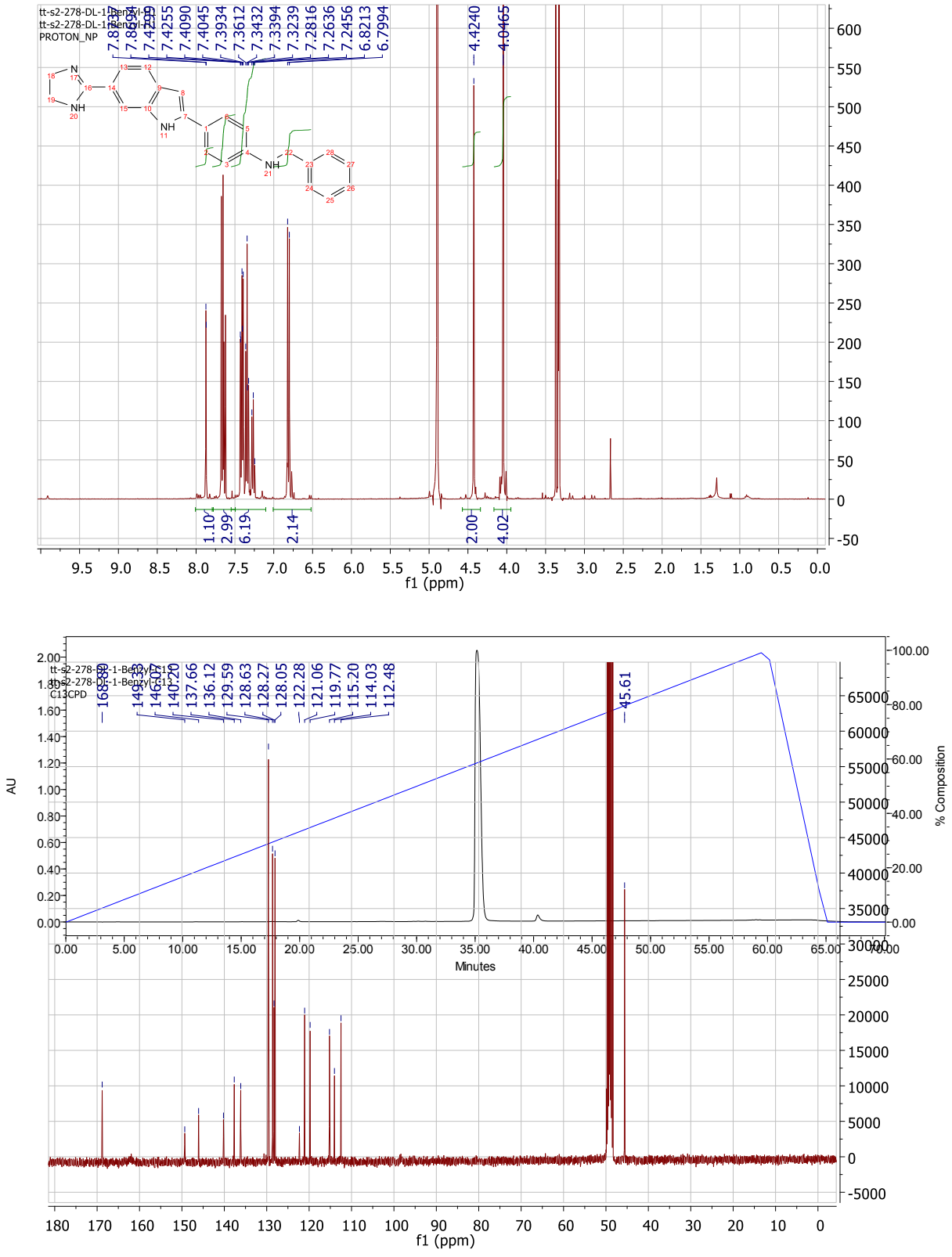

Supplementary Figure S21: ^{1}H NMR spectrum, ^{13}C NMR spectrum and analytical HPLC of **DL-1 Benzyl.** The purity of **DL-1 Benzyl** was determined by reverse phase HPLC using a

gradient of 0-100% MeOH in water over 60 min; t_R= 35 min. MS-ESI(+) HRMS: calculated: 367.1917 ($M + H^+$); observed: 367.1921 ($M + H^+$). ^{1}H NMR (MeOH-D_4, 400 MHz) δ 4.07 (4H, s), 4.44 (2H, s), 6.85 (2H, d, J= 9 Hz), 7.28 (1H, m) 7.35 (2H, m), 7.42 (3H, m), 7.65 (1H, d, J= 8 Hz), 7.69 (2H, d, J= 9 Hz), 7.89 (1H, s). ^{13}C NMR (MeOH-D_4, 100 MHz) δ 45.61, 49.87, 112.48, 124.03, 115.20, 119.77, 121.06, 122.28, 128.05, 128.27, 128.63, 129.59, 136.12, 137.66, 140.20, 146.07, 149.33, 168.80.

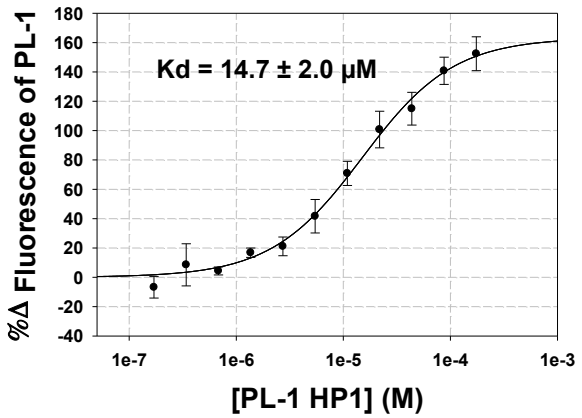
Kd = 14.7 ± 2.0 µM
%Δ Fluorescence of PL-1
[PL-1 HP1] (M)

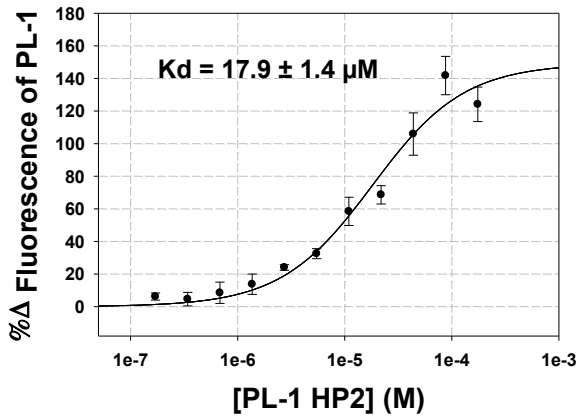
Kd = 17.9 ± 1.4 µM
%Δ Fluorescence of PL-1
[PL-1 HP2] (M)

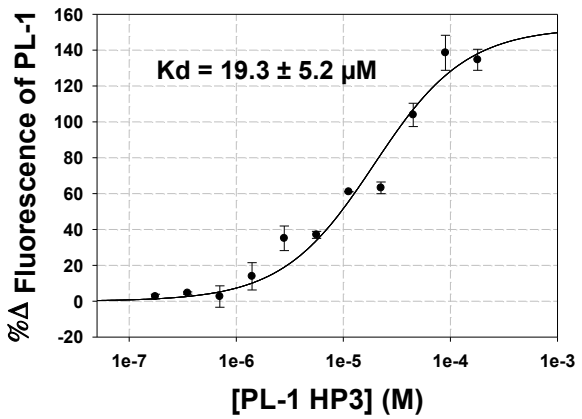
Kd = 19.3 ± 5.2 µM
%Δ Fluorescence of PL-1
[PL-1 HP3] (M)

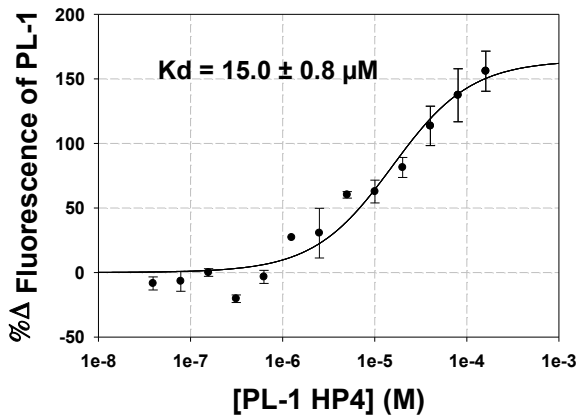
Kd = 15.0 ± 0.8 µM
%Δ Fluorescence of PL-1
[PL-1 HP4] (M)

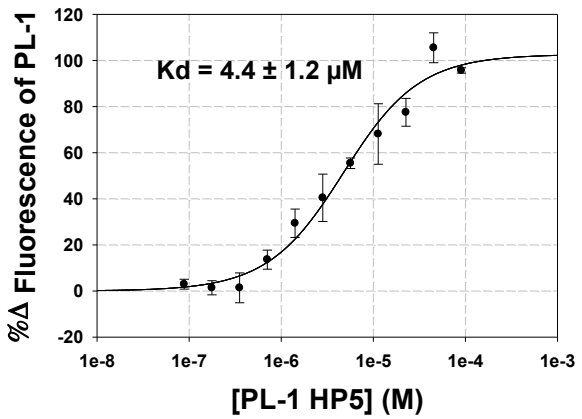
Kd = 4.4 ± 1.2 µM
%Δ Fluorescence of PL-1
[PL-1 HP5] (M)

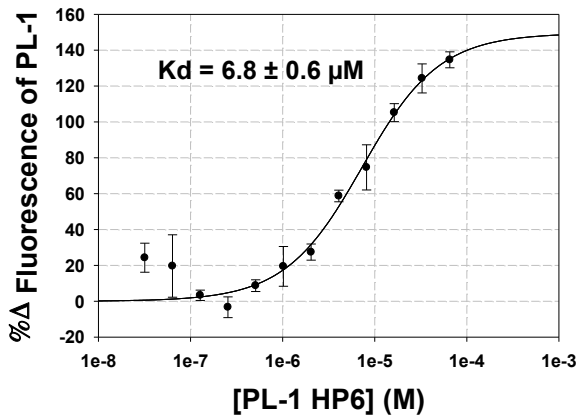
Kd = 6.8 ± 0.6 µM
%Δ Fluorescence of PL-1
[PL-1 HP6] (M)

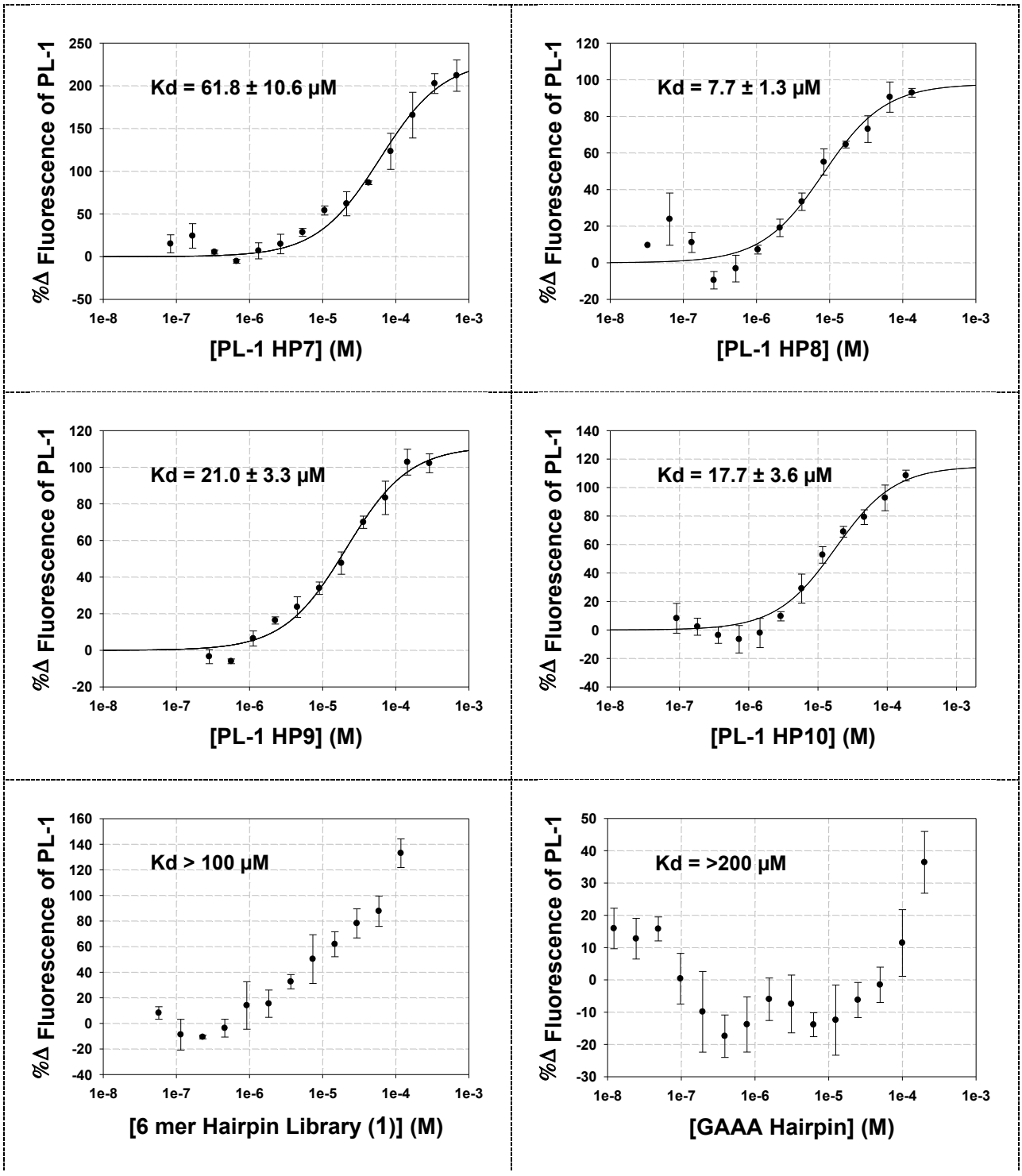

Supplementary Figure S22: Binding curves of selected RNAs to **PL-1.** Each experiment was completed in triplicate and the error bars are the standard deviations.

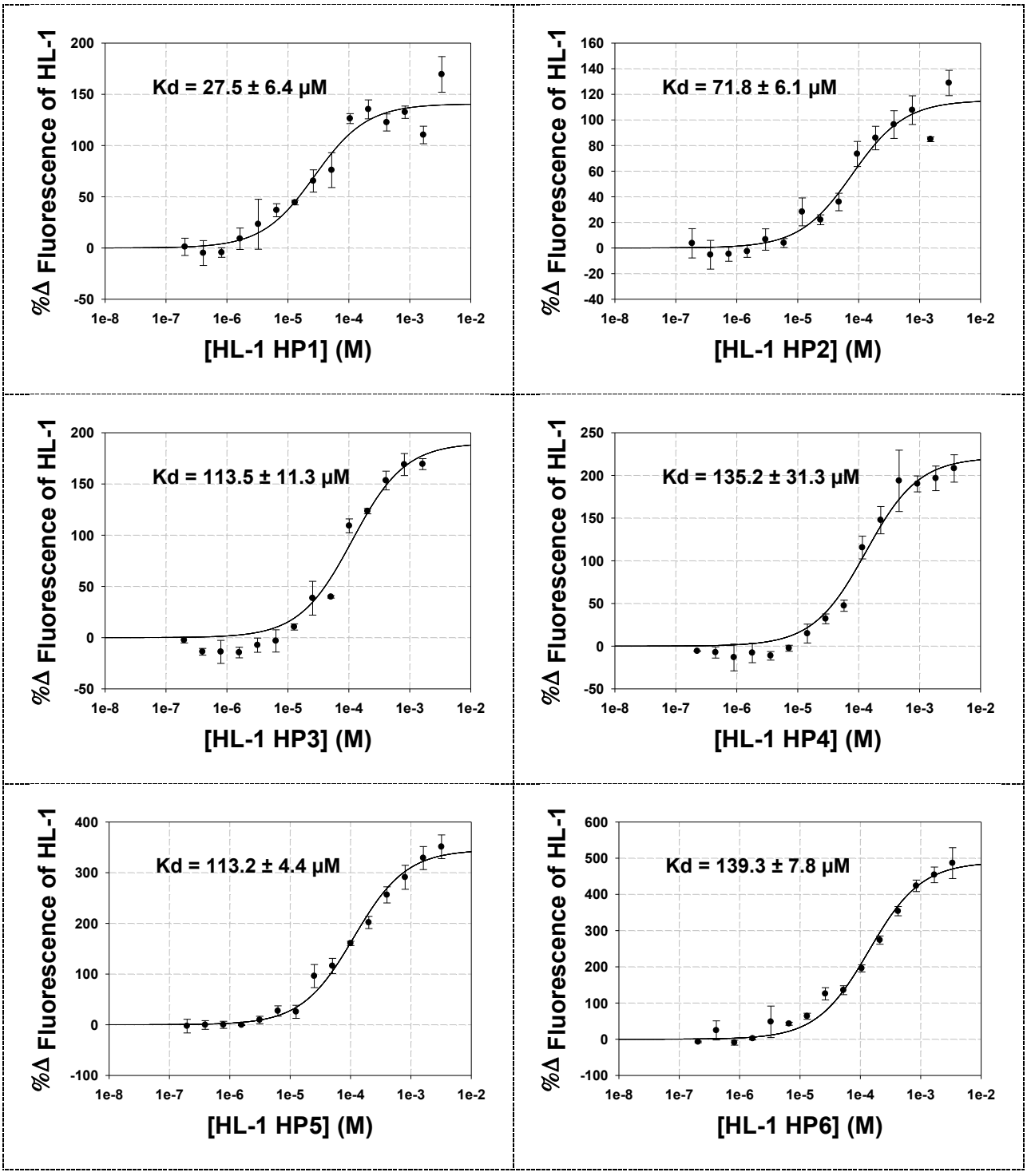
Kd = 27.5 ± 6.4 µM
%Δ Fluorescence of HL-1
[HL-1 HP1] (M)
Kd = 71.8 ± 6.1 µM
%Δ Fluorescence of HL-1
[HL-1 HP2] (M)
Kd = 113.5 ± 11.3 µM
%Δ Fluorescence of HL-1
[HL-1 HP3] (M)
Kd = 135.2 ± 31.3 µM
%Δ Fluorescence of HL-1
[HL-1 HP4] (M)
Kd = 113.2 ± 4.4 µM
%Δ Fluorescence of HL-1
[HL-1 HP5] (M)
Kd = 139.3 ± 7.8 µM
%Δ Fluorescence of HL-1
[HL-1 HP6] (M)

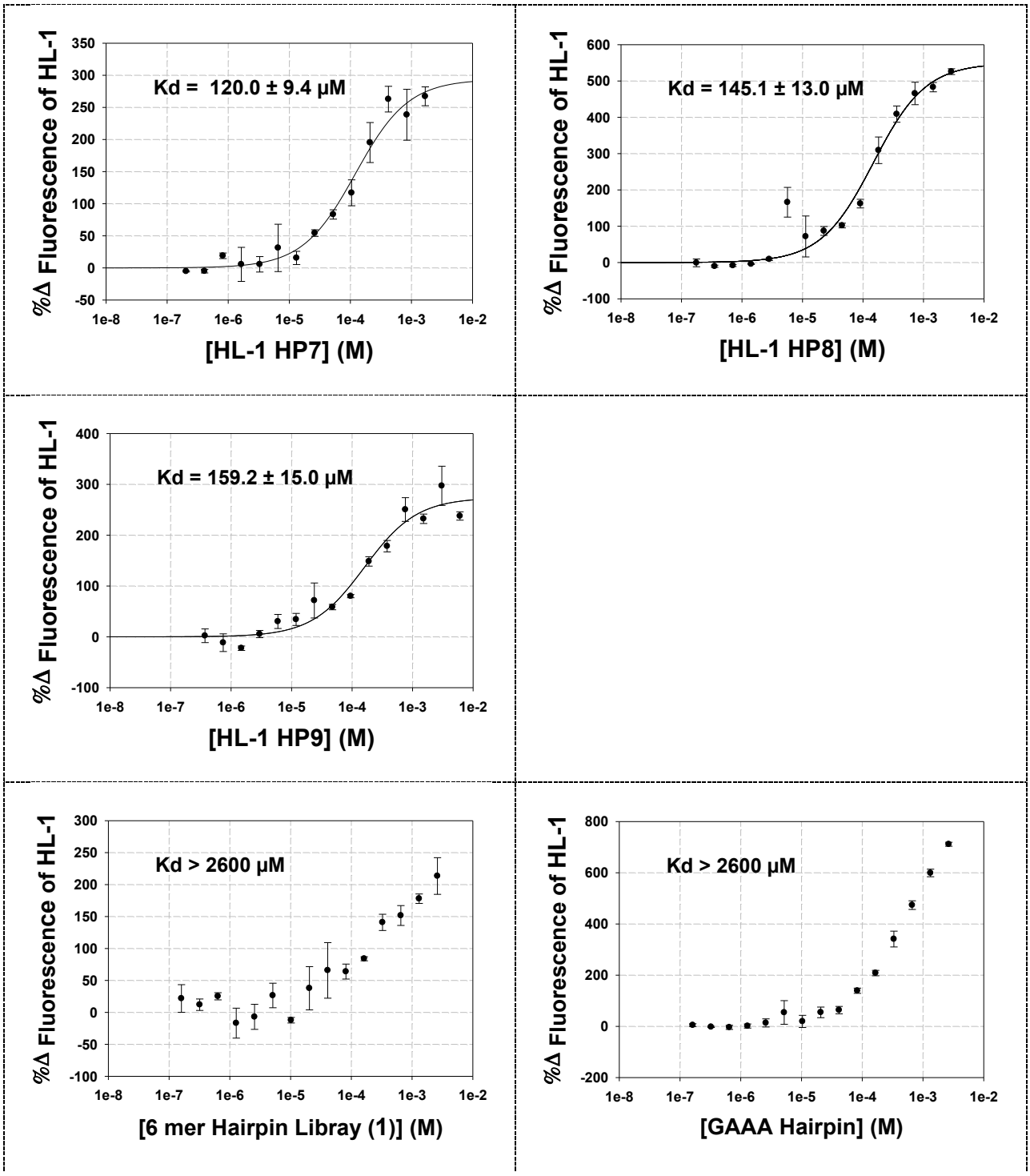

Supplementary Figure S23: Binding curves of selected RNAs to **HL-1.** Each experiment was completed in triplicate and the error bars are the standard deviation from triplicate experiments.

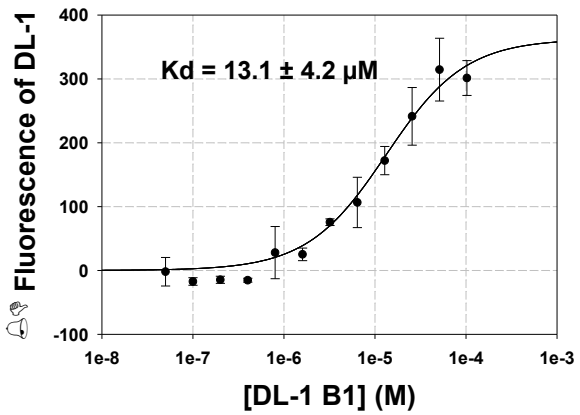
Kd = 13.1 ± 4.2 μM
Fluorescence of DL-1
[DL-1 B1] (M)

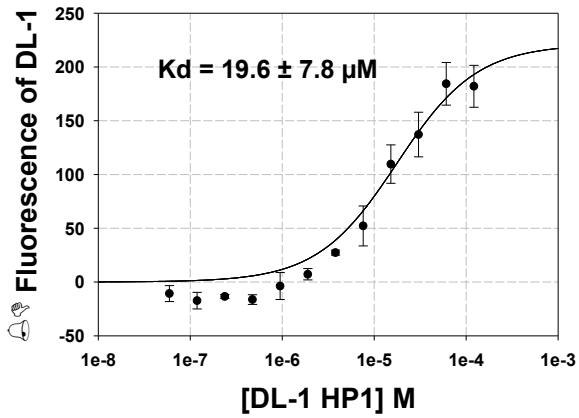
Kd = 19.6 ± 7.8 μM
Fluorescence of DL-1
[DL-1 HP1] M

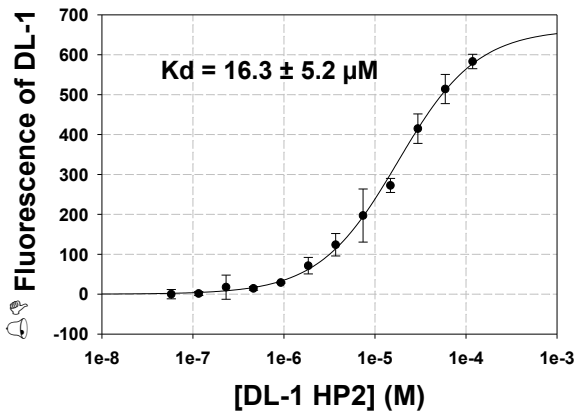
Kd = 16.3 ± 5.2 μM
Fluorescence of DL-1
[DL-1 HP2] (M)

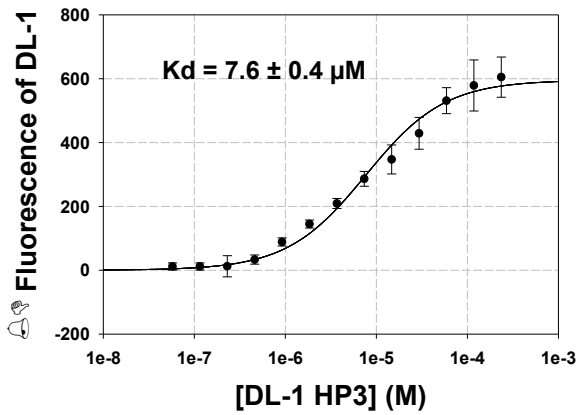
Kd = 7.6 ± 0.4 μM
Fluorescence of DL-1
[DL-1 HP3] (M)

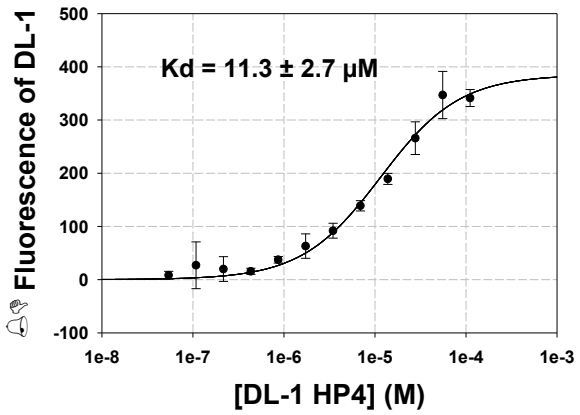
Kd = 11.3 ± 2.7 μM
Fluorescence of DL-1
[DL-1 HP4] (M)

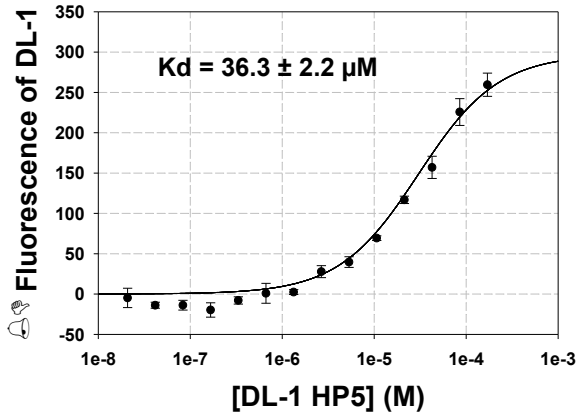
Kd = 36.3 ± 2.2 μM
Fluorescence of DL-1
[DL-1 HP5] (M)

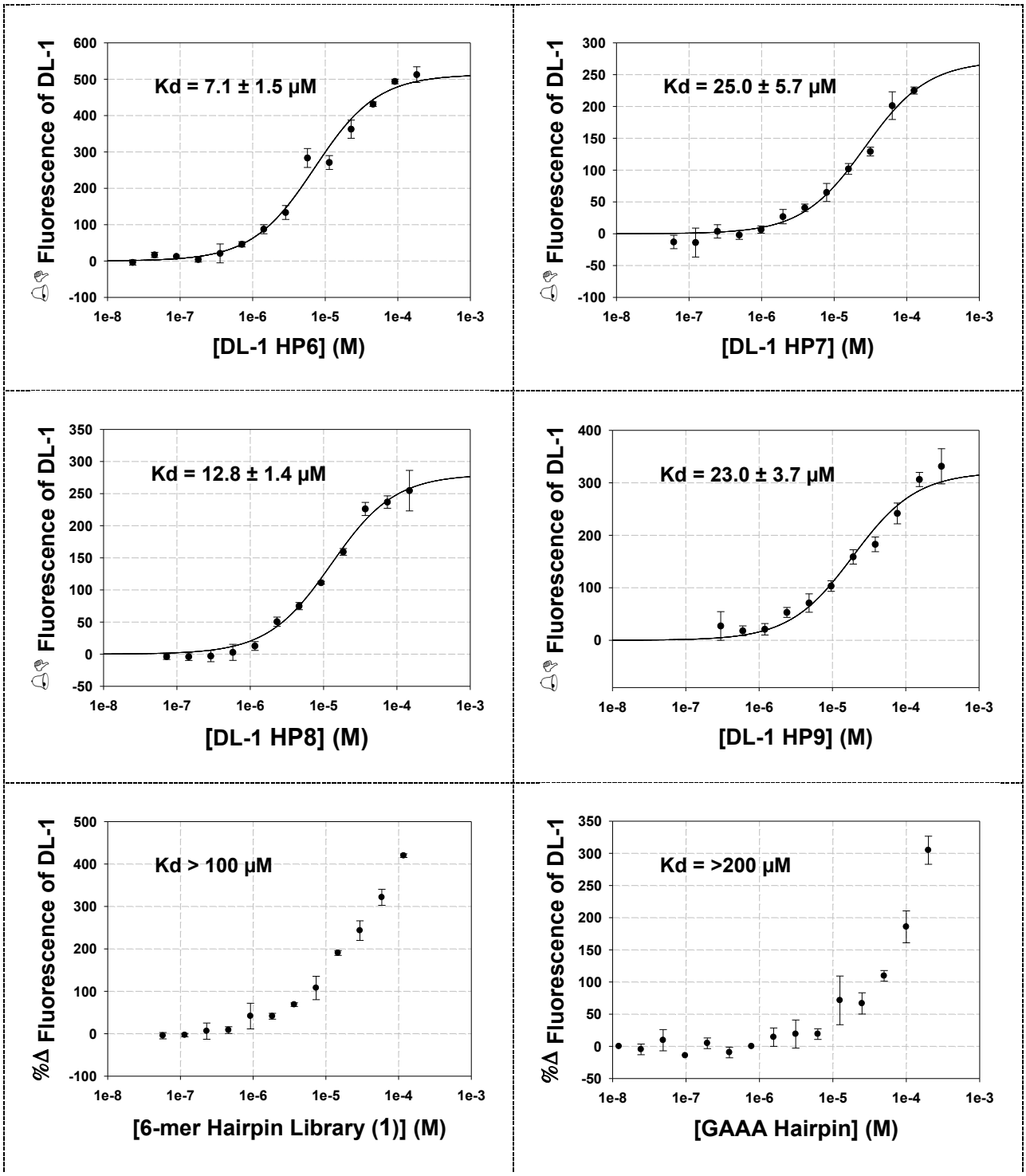

Supplementary Figure S24: Binding curves of selected RNAs to **DL-1.** Each experiment was completed in triplicate and the error bars are the standard deviations.

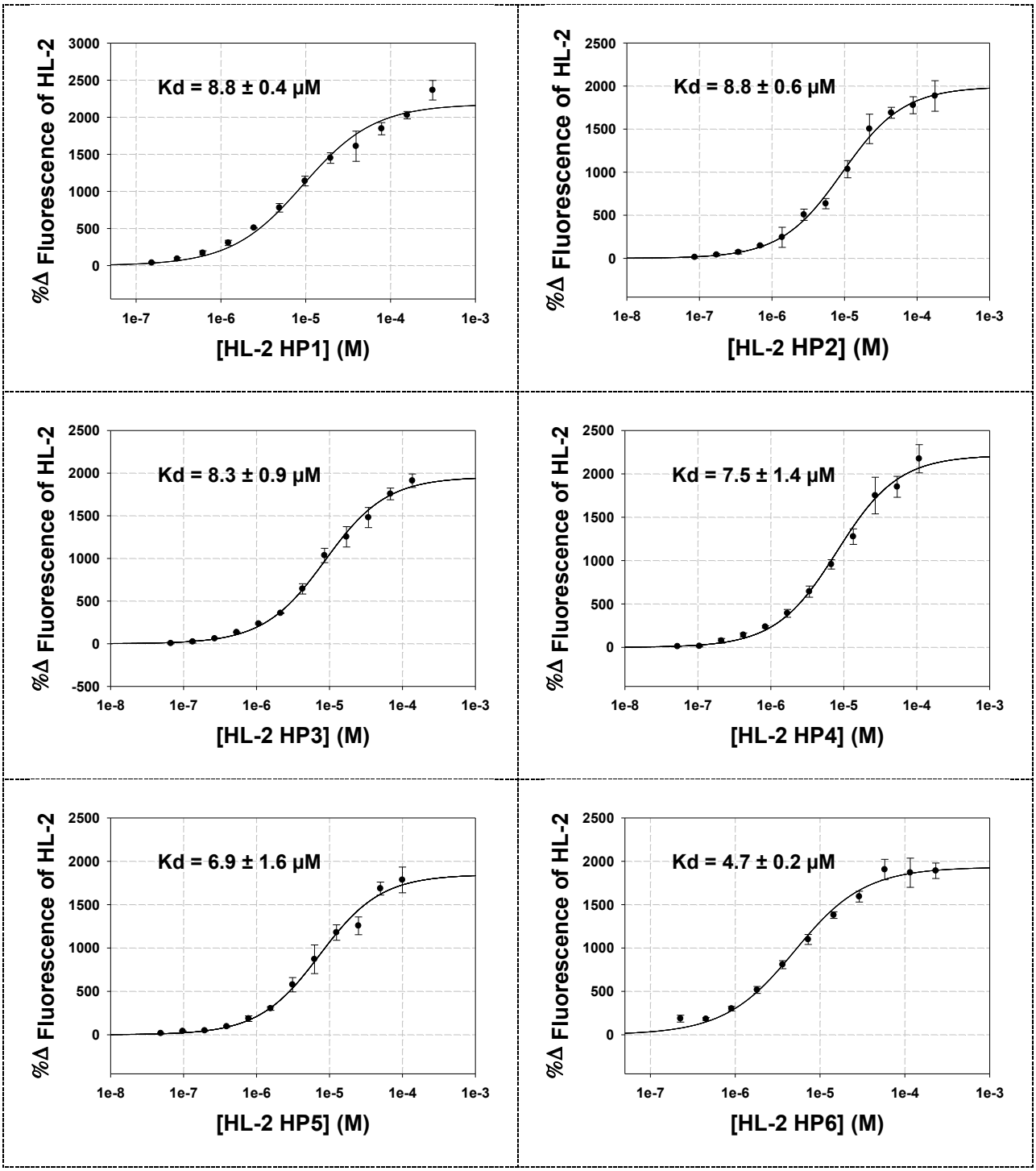
Kd = 8.8 ± 0.4 µM
%Δ Fluorescence of HL-2
[HL-2 HP1] (M)
Kd = 8.8 ± 0.6 µM
%Δ Fluorescence of HL-2
[HL-2 HP2] (M)
Kd = 8.3 ± 0.9 µM
%Δ Fluorescence of HL-2
[HL-2 HP3] (M)
Kd = 7.5 ± 1.4 µM
%Δ Fluorescence of HL-2
[HL-2 HP4] (M)
Kd = 6.9 ± 1.6 µM
%Δ Fluorescence of HL-2
[HL-2 HP5] (M)
Kd = 4.7 ± 0.2 µM
%Δ Fluorescence of HL-2
[HL-2 HP6] (M)

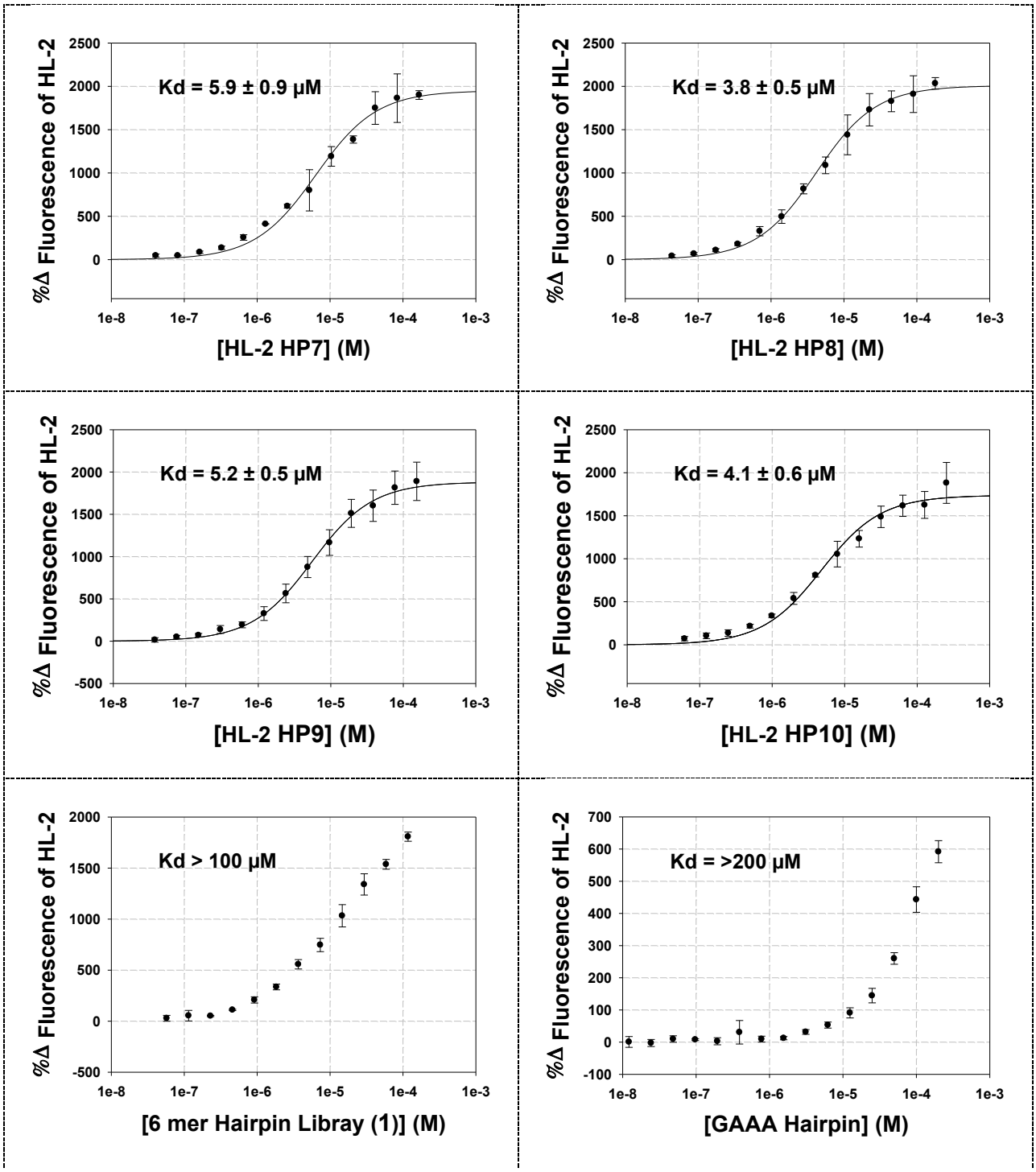

Supplementary Figure S25: Binding curves of selected RNAs to **HL-2.** Each experiment was completed in triplicate and the error bars are the standard deviations.

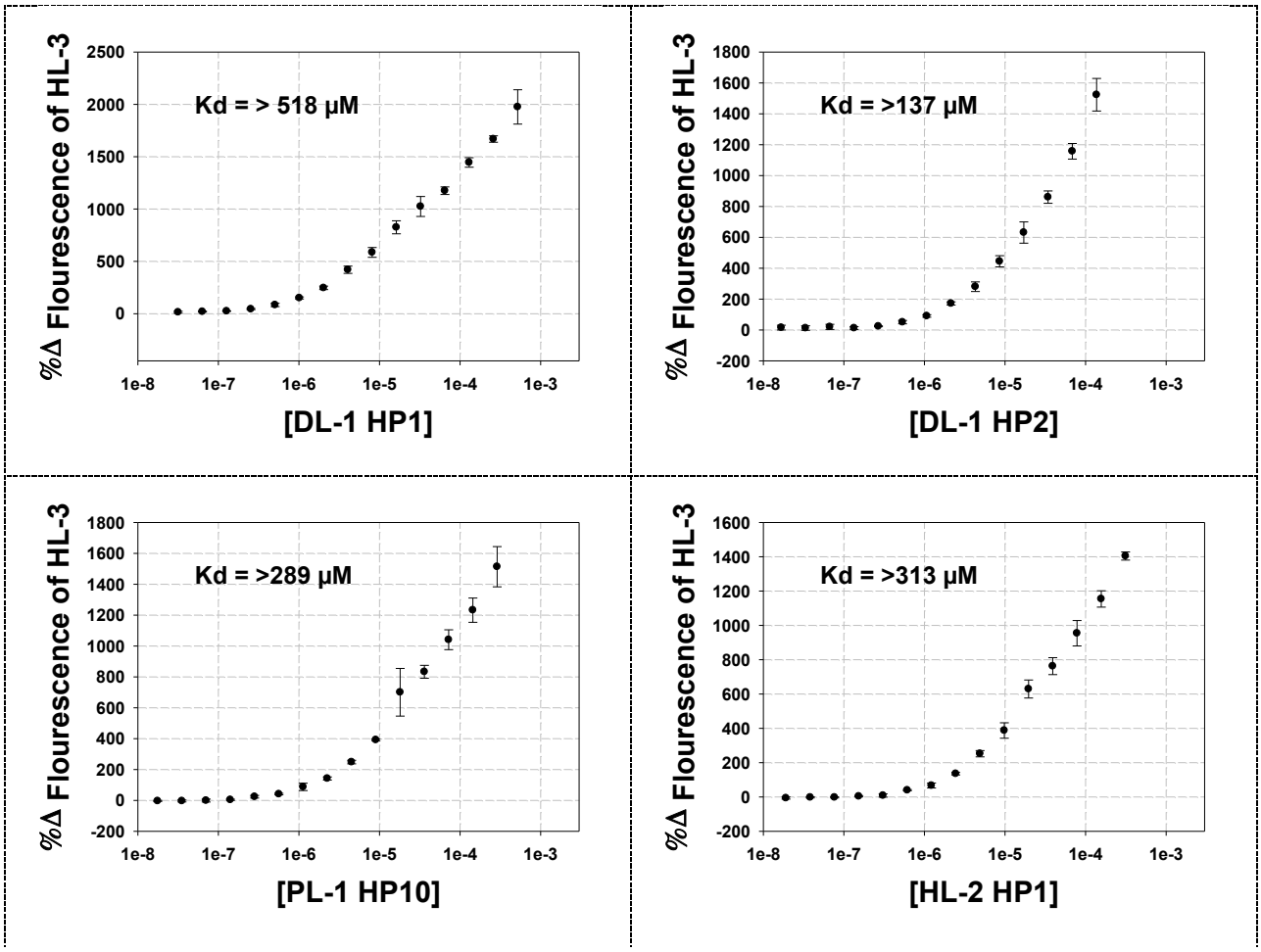

Supplementary Figure S26: Binding curves of RNAs to **HL-3.** Each experiment was completed in triplicate and the error bars are the standard deviations.

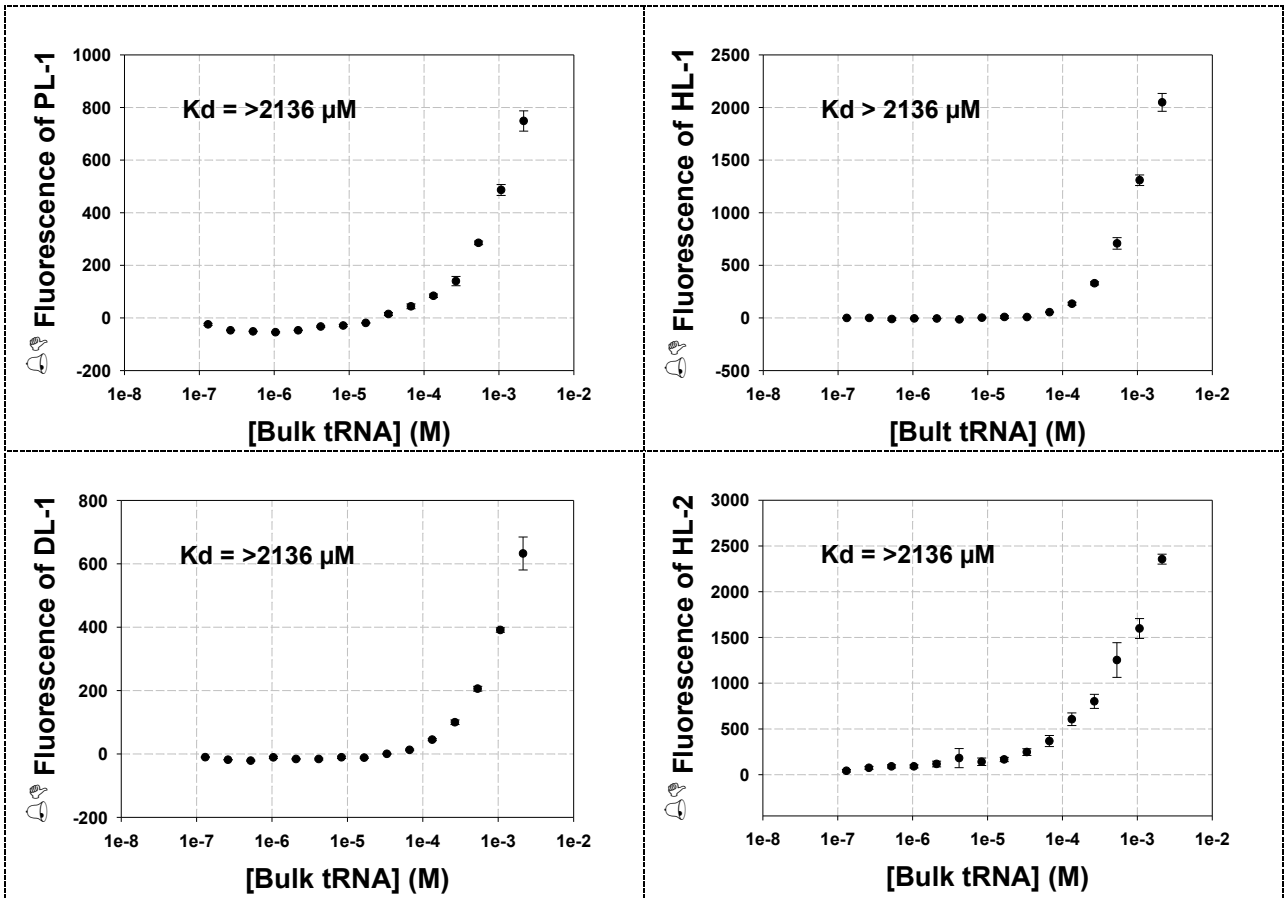

Supplementary Figure S27: Binding curves of bulk tRNA and **DL-1**, **HL-1**, **PL-1** and **HL-2.** Each experiment was completed in triplicate and the error bars are the standard deviations.

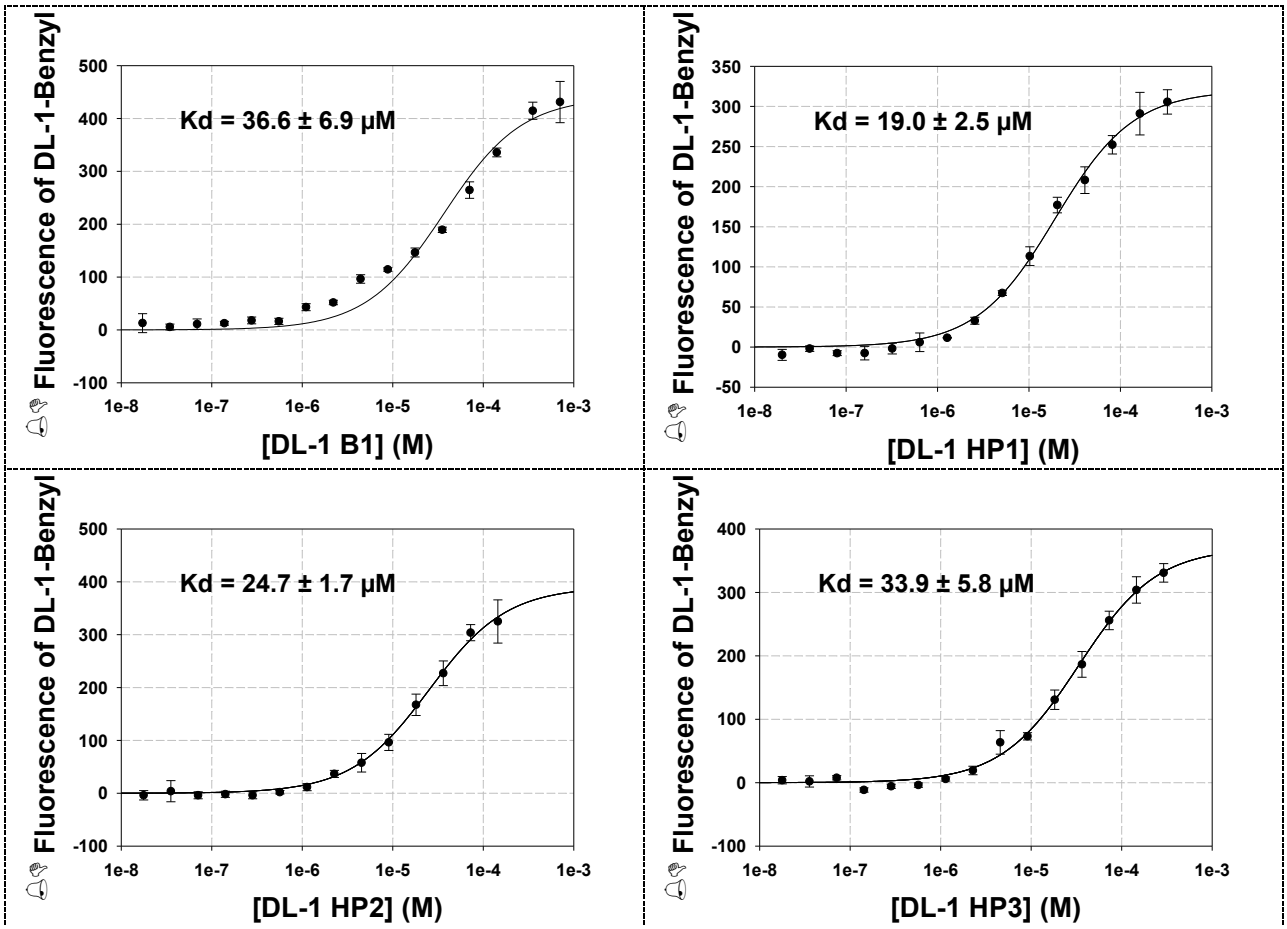

Supplementary Figure S28: Binding curves of RNAs to **DL-1 Benzyl.** Each experiment was completed in triplicate and the error bars are the standard deviations.

Supplementary Table S1: Small molecules that were used in this study.					
Compound ID	#	Small Molecules Structures	RNA Library **1***	RNA Library **2***	RNA Library **3***
PL-1	**1**	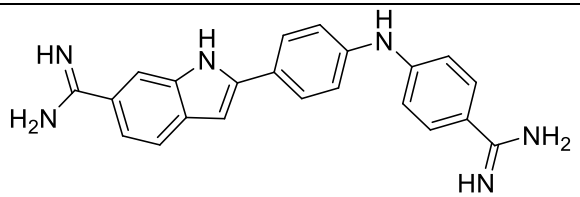 Pentamidine - like	9.3±0.5	8.3±0.1	10.4±0.5
HL-1	**2**	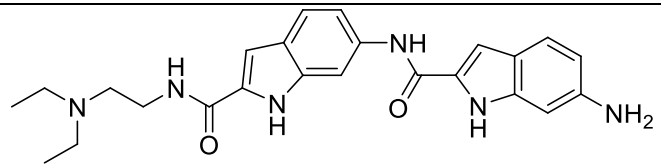 Hoechst - like	23.6±2.8	16.2±0.5	34.8±2.2
DL-1	**4**	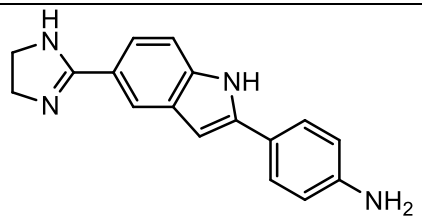 DAPI - like	36.9±0.7	20.7±0.5	26.3±0.4
HL-2	**8**	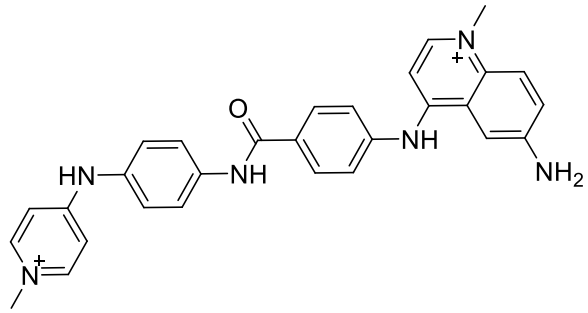 Hoechst - like	62.8±6.5	59.7±3.5	79.3±0.0

HL-3	**3**	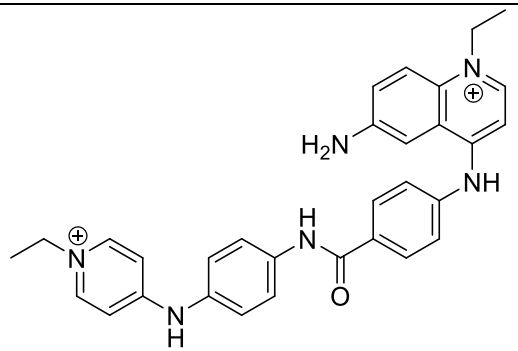 Hoechst - like	26.8±1.9	32.4±2.0	57.1±3.1
DL-2	**5**	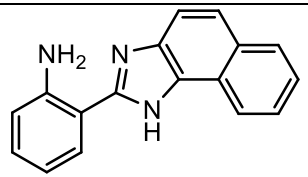 DAPI - like	45.9±0.7	37.9±0.8	40.7±2.8
DL-3	**6**	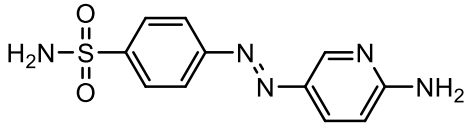 DAPI - like	60.6±0.7	47.5±2.1	57.6±0.4
HL-4	**7**	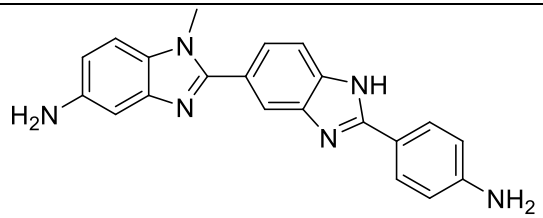 Hoechst - like	44.9±1.8	46.3±1.4	51.8±0.7

HL-5	**9**	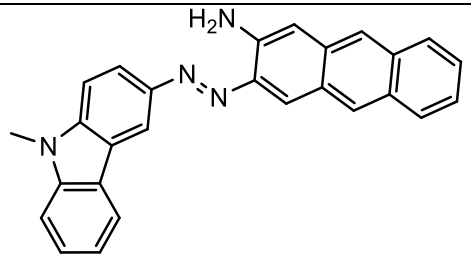 Hoechst - like	80.1±2.3	73.0±1.1	78.1±2.7
PL-2	**10**	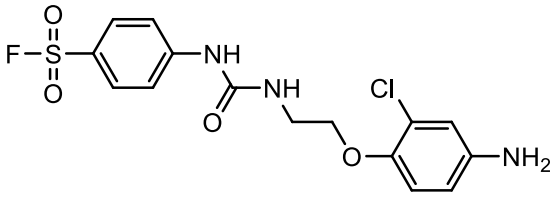 Pentamidine - like	80.4±3.2	74.3±4.3	76.7±3.6
DL-4	**11**	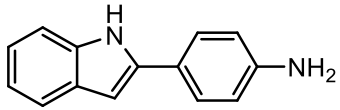 DAPI - like	82.4±3.4	81.2±1.1	83.4±1.8
HL-6	**12**	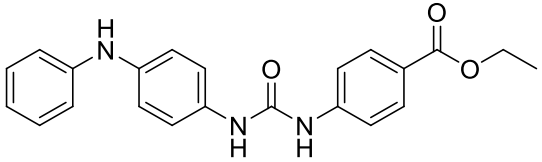 Hoechst - like	84.3±1.1	86.5±0.4	84.0±0.3
DL-5	**13**	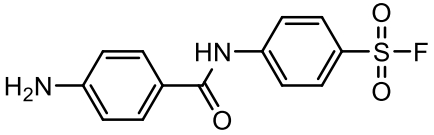 DAPI - like	84.8±0.9	88.5±2.7	88.7±2.7

HL-7	**14**	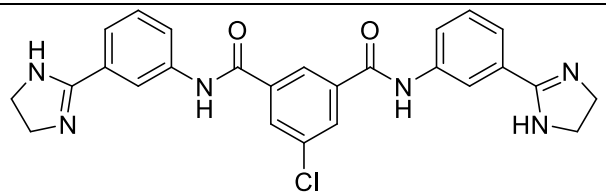 Hoechst - like	84.8±1.9	56.9±3.6	85.8±4.2
PL-3	**15**	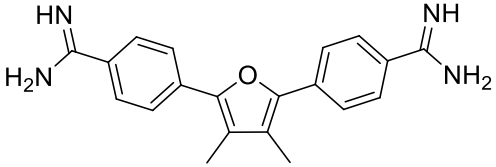 Pentamidine - like	87.3±4.2	113.0±19.6	110.7±7.0
HL-8	**16**	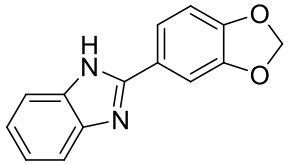 Hoechst - like	87.5±2.6	82.0±1.8	97.1±2.5
HL-9	**17**	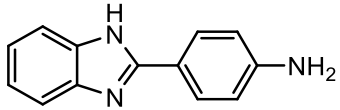 Hoechst - like	90.1±1.9	69.9±1.3	81.1±3.2
HL-10	**18**	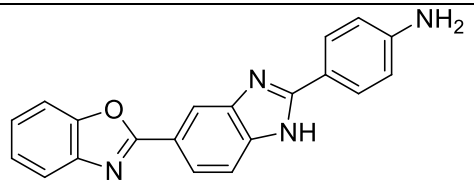 Hoechst - like	90.9±0.7	87.8±0.4	90.1±1.4
DL-6	**19**	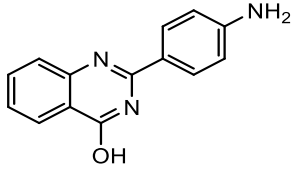 DAPI - like	90.9±2.5	82.6±1.2	90.3±2.8

PL-4	**20**	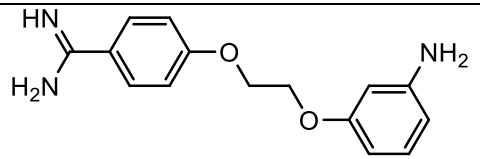 Pentamidine - like	92.0±2.2	88.9±3.0	95.4±2.0
PL-5	**21**	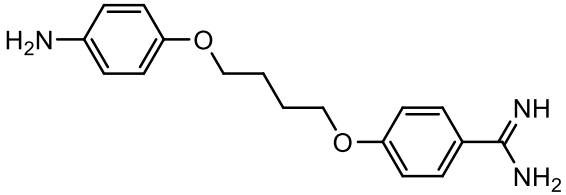 Pentamidine - like	93.0±1.4	87.6±3.3	91.2±3.7
PL-6	**22**	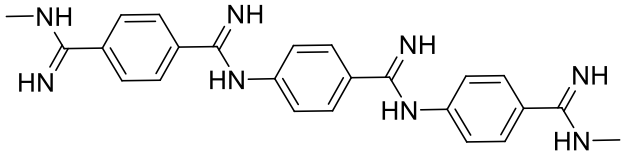 Pentamidine - like	93.2±1.3	90.0±2.1	95.9±1.9
HL-11	**23**	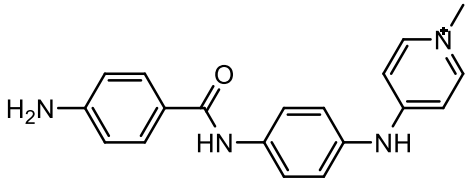 Hoechst - like	93.8±2.9	96.7±1.6	99.0±1.6
DL-7	**24**	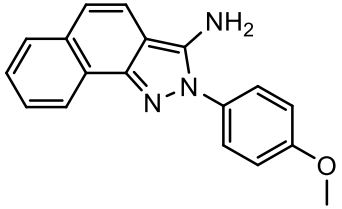 DAPI - like	94.8±1.7	91.0±2.6	91.1±1.9

HL-12	**25**	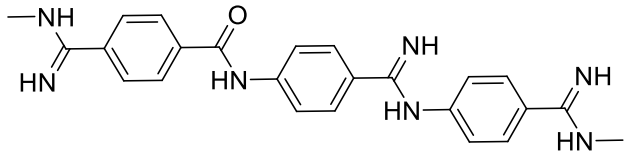 Hoechst - like	94.9±0.7	87.8±3.3	95.0±3.4
HL-13	**26**	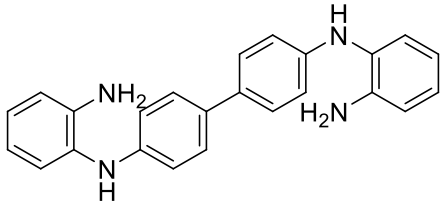 Hoechst - like	95.1±1.7	98.1±1.1	99.0±1.1
PL-7	**27**	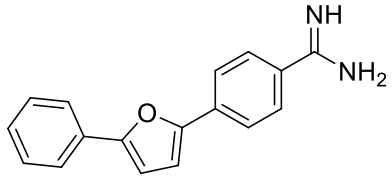 Pentamidine - like	95.5±1.4	72.5±1.4	97.5±3.4
PL-8	**28**	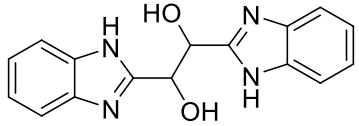 Pentamidine - like	96.6±2.1	99.1±2.0	101.5±0.8
HL-14	**29**	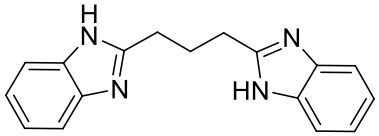 Hoechst - like	98.0±0.8	99.4±0.5	100.3±1.2
PL-9	**30**	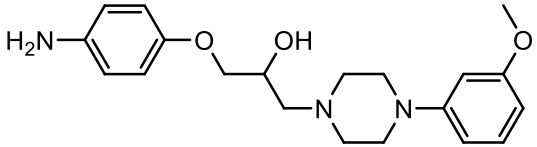 Pentamidine - like	98.4±1.8	92.7±1.5	94.6±2.5

PL-10	**31**	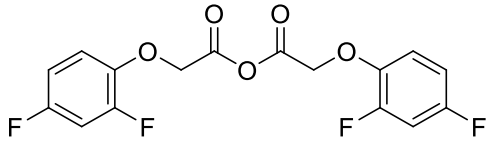 Pentamidine - like	99.1±2.1	104.3±0.7	103.4±0.8
HL-15	**32**	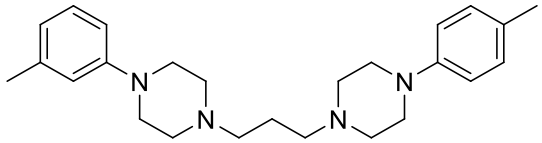 Hoechst - like	99.2±1.2	100.7±0.3	101.2±1.0
HL-16	**33**	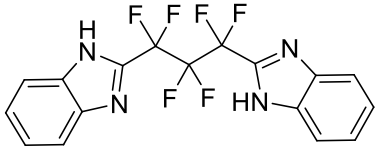 Hoechst - like	100.0±1.0	101.3±1.4	100.7±1.2
HL-17	**34**	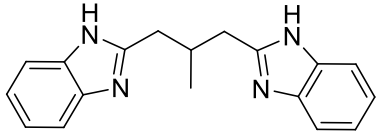 Hoechst - like	100.1±0.8	95.1±1.3	93.9±1.8
PL-11	**35**	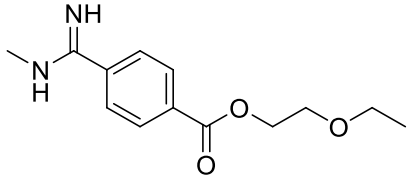 Pentamidine - like	100.1±1.5	103.7±3.6	104.4±0.8
PL-12	**36**	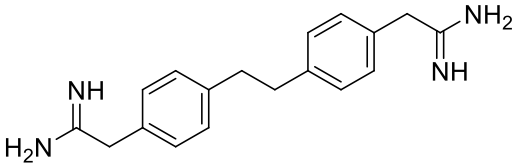 Pentamidine - like	101.1±0.8	102.1±2.0	104.4±2.5

HL-18	**37**	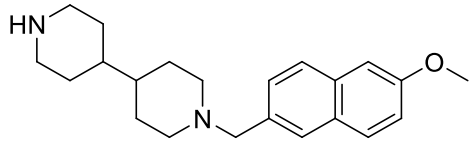 Hoechst - like	102.1±1.1	86.5±2.7	100.2±0.4
HL-19	**38**	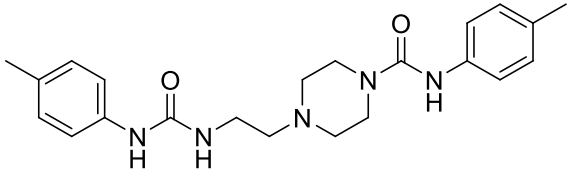 Hoechst - like	102.3±0.7	97.4±0.7	100.4±0.1
HL-20	**39**	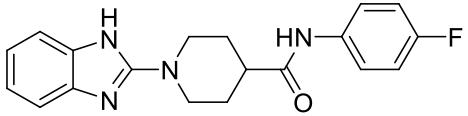 Hoechst - like	104.5±1.0	103.1±1.1	104.3±0.9
PL-13	**40**	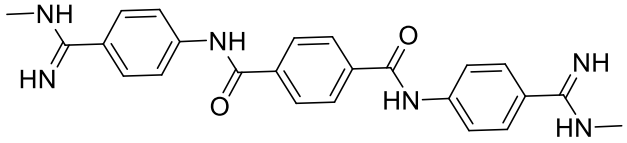 Pentamidine - like	106.2±3.2	88.2±4.9	105.8±2.0
HL-21	**41**	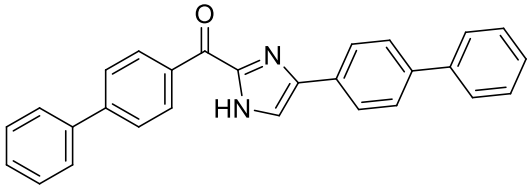 Hoechst - like	107.1±1.8	108.3±4.8	106.6±2.0
PL-14	**42**	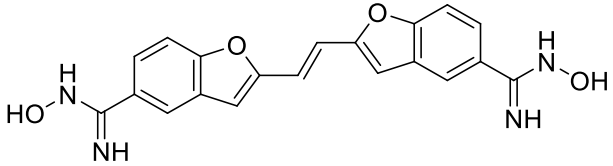 Pentamidine - like	115.4±3.3	125.4±2.8	122.0±2.8

DL-8	**43**	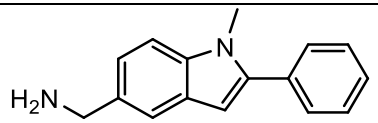 DAPI - like	138.0±2.0	88.8±1.9	96.6±2.5
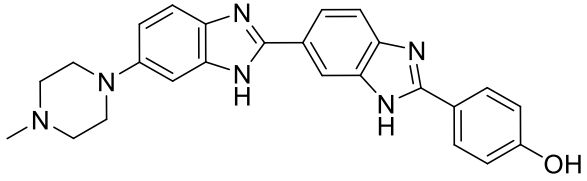 Hoechst 33258		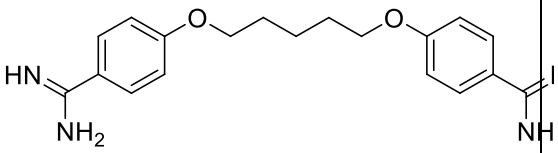 Pentamidine		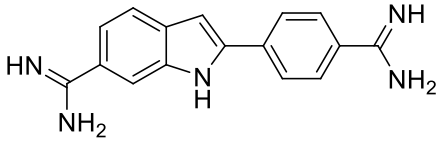 4',6'-diamidino-2-phenylindole (DAPI)	
PL represents pentamidine-like, HL represents Hoechst-like and DL represents DAP- like * % change in fluorescence intensity of TO-PRO-1 from the displacement assay.					

Supplementary Table S2: Number of sequences obtained for each RNA library				
RNA Library	**1**	**2**	**3**	Total RNA sequenced
Starting Library	37	47	21	105
PL-1 Selected RNAs	40	8	0	48
HL-1 Selected RNAs	42	4	0	46
DL-1 Selected RNAs	32	14	0	46
HL-2 Selected RNAs	22	3	0	25

Supplementary Methods

*Instrumentation***.** NMR spectra were collected using a Bruker NMR spectrometer operating at 400 MHz on proton. Chemical shifts were referenced to residual solvent or an internal trimethyl silane (TMS) standard. Mass spectra were collected on LQT mass spectrometer (Thermo Scientific, Pittsburgh, PA). HPLC traces were collected on a Waters 1525 binary HPLC pump equipped with Waters 2487 Dual Absorbance Detector system. Radioactive gels were exposed to phosphorimager screens and imaged with a Typhoon 9410 variable mode imager (Molecular Dynamics). Images were quantified with QuantityOne software (BioRad). The pH of buffers was measured at room temperature using a Mettler Toledo SG2 pH meter that was standardized at pH 4.0, 7.0, and 10.0. An Aurora Discovery FRD-1B liquid dispenser was used to deliver liquid into 384-well plates. A Biomek NX^P Laboratory Automation Workstation (Beckman Coulter) that was equipped with 384-pin head (100 nL delivery) was used to deliver the ligands to 384-well plates. An Envision 2104 multilabel plate reader (Perkin Elmer) and a FLx800 fluorescence microplate reader (Bio-Tek) were used to measure fluorescence intensity of TO-PRO-1 or compounds in affinity measurements.

*Chemicals***.** All small molecules used in the high throughput screen were acquired from the National Cancer Institute (NCI) and were purified by HPLC prior to downstream MDCS experiments and affinity measurements. The library of pharmaceutically active compounds (LOAC) was procured from Sigma Aldrich and was obtained from the Scripps Research Institute High Throughput Screening Center. TO-PRO-1 (Invitrogen), agarose (Fisher Scientific), HPLC solvents (Sigma Aldrich), sodium cyanoborohydride ($NaBH_3CN$) (Acros Organics), tris(hydroxymethyl)aminomethane (Tris-HCl) (EMD), NaCl (EMD), and

ethylenediamine tetraacetic acid (EDTA) (Fisher Scientific) were used without further purification.

General Nucleic Acids. All DNA oligonucleotides were purchased from Integrated DNA Technologies Inc. (IDT) and used without further purification. The RNA competitor oligonucleotides were purchased from Dharmacon and deprotected according to the manufacturer's standard procedure. All aqueous solutions were made with NANOpure water. The RNA libraries (Figure 2) were embedded in a hairpin cassette [57]. They display randomized regions in a 6-nucleotide hairpin pattern (**1**), a 3×2 nucleotide internal loop pattern (**2**), or a 4×4 nucleotide internal loop pattern (**3**). Libraries **1**, **2** and **3** were synthesized by *in vitro* transcription from the corresponding DNA template that was custom-mixed at the randomized positions to ensure equivalent representation of all four nucleotides.

PCR Amplification of DNA Templates Encoding Selected RNAs. The DNA templates encoding the selected RNAs were purchased from IDT and were PCR amplified to install a T7 promoter. PCR amplification was completed in 50 μL of 1X PCR buffer (10 mM Tris-HCl, pH 9.0, 50 mM KCl, and 0.1% Triton X-100), 4.25 mM $MgCl_2$, 0.33 mM dNTPs, 2 μM each primer (RT primer: 5'-d(CCTTGCGGATCCAAT and PCR primer: 5'-d(GGCCGGATCCTAATACGACTCACTATAGGGAGAGGGTTTAAT), and 0.1 μL of Taq DNA polymerase. The DNA was amplified by 25 cycles of 95 ^{o}C for 30 s, 50 ^{o}C for 30 s, and 72 ^{o}C for 1 min. All PCR reactions were checked by gel electrophoresis on a 5% agarose gel stained with ethidium bromide.

RNA Transcription and Purification. RNA oligonucleotides were transcribed as described previously described [20, 49, 50, 52-54, 58]. Briefly, transcription was completed using an RNAMaxx transcription kit (Stratagene) according to the manufacturer's protocol using 12.5 μL of the amplified DNA template from a PCR reaction or 1 pmole of DNA template purchased from IDT. After transcription, 1 unit of DNase I (Invitrogen) was added, and the sample was incubated at 37 °C for additional 30 min. Transcribed RNAs were then purified by gel electrophoresis on a denaturing 15% polyacrylamide gel. The RNAs were visualized by UV shadowing and extracted into 300 mM NaCl by tumbling overnight at 4 °C. The resulting solution was concentrated with 2-butanol, and the RNA was ethanol precipitated. The RNAs were re-suspended in 150 μL of NANOpure water, and the concentrations were determined by the absorbance at 260 nm and the corresponding extinction coefficient. Oligonucleotide extinction coefficients were determined using HyTher version 1.0 (Nicolas Peyret and John SantaLucia Jr., Wayne State University, Detroit, MI) [60, 61]. These parameters were calculated from information on the extinction coefficients of nearest neighbors in RNA [62].

Supplementary References

60 Peyret, N., Seneviratne, P. A., Allawi, H. T. & SantaLucia, J., Jr. Nearest-neighbor thermodynamics and NMR of DNA sequences with internal A.A, C.C, G.G, and T.T mismatches. *Biochemistry* **38**, 3468-3477 (1999).

61 SantaLucia, J., Jr. A unified view of polymer, dumbbell, and oligonucleotide DNA nearest-neighbor thermodynamics. *Proc. Natl. Acad. Sci. U. S. A.* **95**, 1460-1465 (1998).

62 Puglisi, J. D., Tinoco, I., James, E. D. & John, N. A. in *Methods Enzymol.* **180**, 304-325 (1989).